10-11-2018

An Expanded Modern Coexistence Theory for Empirical Applications

Stephen P. Ellner
Cornell University

Robin E. Snyder
Case Western Reserve University

Peter B. Adler
Utah State University

Giles J. Hooker
Cornell University

Recommended Citation

Ellner, S. P., Snyder, R. E., Adler, P. B. and Hooker, G. (2018), An expanded modern coexistence theory for empirical applications. Ecol Lett. . doi:10.1111/ele.13159

An Expanded Modern Coexistence Theory for Empirical Applications

Stephen P. Ellner*[a], Robin E. Snyder[b], Peter B. Adler[c] and Giles J. Hooker[d]

[a]Department of Ecology and Evolutionary Biology, Cornell University, Ithaca, New York
[b]Department of Biology, Case Western Reserve University, Cleveland, Ohio
[c]Department of Wildland Resources and the Ecology Center, Utah State University, Logan, Utah
[d]Department of Biological Statistics and Computational Biology, Cornell University, Ithaca, New York

August 12, 2018

Keywords: Coexistence, competition, environmental variability, model, theory.

Running title: Extending Coexistence Theory

Article type: Ideas and Perspectives
Words in Abstract: 200
Words in main text: 6857 (TeXcount, `http://app.uio.no/ifi/texcount`)
Words in text boxes: 486 (main text + text boxes = 7343)
Number of references: 46
Number of figures: 3
Number of tables: 6
Number of text boxes: 1

Authorship statement: SPE, RES and GJH led the theory development; SPE and PBA led the data analysis and modeling; SPE, PBA and RES wrote scripts to simulate and analyze models; all authors discussed all aspects of the research and contributed to writing and revising the paper.

Data accessibility statement: No original data appear in this paper. Should the paper be accepted, all computer scripts supporting the results will be archived in an appropriate public repository such as Dryad or Figshare, with the DOI included at the end of the article.

*Corresponding author. Department of Ecology and Evolutionary Biology, E145 Corson Hall, Cornell University, Ithaca NY 14853-2701. Email: spe2@cornell.edu Phone: 607-254-4221 FAX: 607-257-8088

Abstract Understanding long-term coexistence of numerous competing species is a long-standing challenge in ecology. Progress requires determining which processes and species differences are most important for coexistence when multiple processes operate and species differ in many ways. Modern coexistence theory (MCT), formalized by Chesson, holds out the promise of doing that, but empirical applications remain scarce. We argue that MCTs mathematical complexity and subtlety have obscured the simplicity and power of its underlying ideas and hindered applications. We present a general computational approach that extends our previous solution for the storage effect to all of standard MCTs spatial and temporal coexistence mechanisms, and also process-defined mechanisms amenable to direct study such as resource partitioning, indirect competition, and life history trade-offs. The main components are a method to partition population growth rates into contributions from different mechanisms and their interactions, and numerical calculations in which some mechanisms are removed and others retained. We illustrate how our approach handles features that have not been analyzed in the standard framework through several case studies: competing diatom species under fluctuating temperature, plant-soil feedbacks in grasslands, facilitation in a beach grass community, and niche differences with independent effects on recruitment, survival and growth in sagebrush steppe.

Introduction

Understanding the indefinite coexistence of numerous competing species is a longstanding, central question in community ecology (e.g., Grubb, 1977; Hubbell, 2001; Hutchinson, 1961, 1959; Shmida & Ellner, 1984). This issue is particularly acute for plants, which as Grubb (1977, p.107) noted "all need light, carbon dioxide, water and the same mineral nutrients." But it also arises when co-occuring animal species compete for a resource or habitat that is essential to all, such as coral reef fish competing for territories (e.g., Caley, 1995; Munday, 2004; Sale, 1979; Volkov *et al.*, 2007) and desert rodents competing for seeds (e.g., Abu Baker & Brown, 2014; Brown, 1989; Kotler & Brown, 1988; Ziv *et al.*, 1993)

The solution Grubb proposed was the "regeneration niche": even if the trees are very similar, seeds and seedlings may be very different. Moreover, species may regenerate at different times (e.g., Usinowicz *et al.*, 2017). But there are many other hypotheses, all with theoretical and many with empirical support, including: predator limitation (Holt & Bonsall, 2017), specialist pathogens (Bagchi *et al.*, 2014; Comita *et al.*, 2014), hydrological niches (Silvertown *et al.*, 1999), resource ratio differences (Dybzinski & Tilman, 2007), spatial environmental variation (Sears & Chesson, 2007), and life history trade-offs (Lönnberg & Eriksson, 2013).

Rarely will only one of these processes be operating in a real species-rich communities. Progress therefore requires more than just identifying which processes that might contribute to coexistence operate in a community. If we observe that two warbler species forage in different parts of the tree, is this crucial for coexistence, or irrelevant because neither species is resource-limited? We need ways to determine which differences and processes are most important when species differ in many ways and multiple processes operate.

Modern coexistence theory (MCT), formalized by Chesson (1994) and Chesson (2000a), holds out the promise of doing exactly that, by quantifying the contributions of different mechanisms to species persistence. The over 2300 citations of Chesson (2000b) – nearly half in the last 5 years – attest to the conceptual importance of MCT.[1] However, empirical applications of MCT remain scarce. One difficulty for empirical applications is that applying MCT to a new study system often requires a case-specific model, and deriving the necessary formulas for coexistence

[1] Web of Science, accessed April 25 2018.

mechanisms in a new model entails a complex mathematical analysis requiring a deep mathematical understanding of MCT. Annual plants with variable germination are a classic example in MCT (Chesson, 1994), but the first empirical application Angert *et al.* (2009) required a new model, entailing a 17-page mathematical appendix to derive the necessary formulas.

Another challenge is that restrictive assumptions are often used to make the mathematics tractable, which can bias the results. For example Angert *et al.* (2009) assumed that all species are equally affected by competition and that inter- and intra-specific competition were equal in strength for all species. MCT's assumption of small environmental variance is often problematic for empirical applications, because fluctuation-dependent mechanisms only become important when environmental variation is large. Mathematical results are also largely limited to unstructured models in which populations are described by total abundance, while many empirical population studies use matrix or integral projection models because there are substantial demographic differences between individuals of different ages or sizes. Similarly, formulas for stabilizing and equalizing components of niche differences have been cited and applied (e.g. Godoy & Levine, 2014, eqns. A.4, A.5) without realizing that they are specific to two-species communities with Lotka-Volterra competition. So while analytic results have yielded important insights, empirical applications often requires less restrictive assumptions.

Finally, MCT analyzes coexistence in terms of a few conceptual "mechanisms" (Box 1). Instead, many ecologists might prefer an analysis focusing on observed processes amenable to direct experimental study, such as resource competition, indirect competition via predators or pathogens, life history tradeoffs or other system-specific processes. Theory with the flexibility to analyze coexistence in terms of multiple species differences and multiple mechanisms, in ways that readily adapt to various study systems, would substantially broaden applicability.

We propose a broad extension of MCT that removes these obstacles. Our previous paper (Ellner *et al.*, 2016) provided a partial solution for one mechanism, the storage effect. The general approach here applies to all the standard MCT coexistence mechanisms, to process-defined mechanisms such as those listed above and any others thought to operate in a community. Our approach is an *extension* of current MCT, not a replacement for it, designed for detailed analysis of particular communities rather than general principles and insights.

In many situations the dominant coexistence mechanisms do not involve temporal fluctuations, so long-term data on population responses to temporal variability is not necessary for applying our approach. And with appropriate data, our approach can also be applied to components of population growth rate, such as survival or fecundity.

We begin by summarizing the core ideas which form the conceptual basis for MCT. For clarity we gloss over some subtleties that become important in applications (a thorough, exact exposition is provided by Barabás *et al.* (2018)). We then introduce our approach through a simple case study, coexistence maintained by variable temperature in an experimental community of two diatom species. Next, we present our general approach, and illustrate it through a series of empirical case studies that include spatial coexistence mechanisms, facilitation, and structured populations with stage-specific niche differences. In all of these cases, we quantify coexistence mechanisms not covered by MCT, though for the diatom case study, we also quantify the traditional MCT mechanisms of storage effect and relative nonlinearity. R scripts to replicate all figures and tables are available online (see Data Accessibility Statement).

Core ideas of MCT

MCT posits that coexistence is stabilized by processes that give any species, when rare, a population growth rate advantage over other "resident" species that remain at typical steady-state abundances. A species' average instantaneous population growth rate when rare is called its *invasion growth rate*. A positive invasion growth rate buffers a species against extinction, maintaining its persistence in the community. If a species relies on different resources than its competitors, or is limited by different enemies or different environmental conditions, then its invasion growth rate may be positive. All species persist and coexistence is stable if *all species have a positive invasion growth rate*.

MCT quantifies coexistence mechanisms by asking how they contribute to each invader's population growth rate advantage over resident species. It does this by comparing observed population growth rates with those that would occur if one or more mechanisms were absent. How much would invader and resident growth rates change if all enemies were perfect generalists, or if the environment were constant?

The core approach in MCT is *decompose and compare*. Decompose population growth rates into a sum of terms for the effects of different factors, and then compare invader and residents term-by-term. Considering invader-resident differences is essential because we want to say that a mechanism stabilizes coexistence of species A and species B if it gives each, when it is rare, an advantage over the other. This can happen two ways: the mechanism can help whichever species is rare, or it can hurt whichever species is common. The invader's growth rate includes only the former; to capture both we need to make an invader-resident comparison. A residents' average population growth rate is necessarily zero, because they are neither increasing nor decreasing in the long run. However the contribution of any particular mechanism to that growth rate (e.g., the effect on its growth rate of predator switching or a variable environment) could be positive or negative, depending on whether the mechanism helps or hurts.

Standard MCT uses Taylor-series expansions to decompose and to evaluate invader-resident differences; in sec. SI.1 we give a simple example to illustrate the procedures. The resulting term-by-term differences in the growth rate decomposition are then grouped into the canonical coexistence mechanisms of standard MCT (Box 1).

In the invader-resident comparisons, it is essential that residents are not allowed to re-equilibrate when we ask, for example, how does variance in temperature contribute to coexistence? It seems natural to answer that question by doing a simulation or experiment with temperature held constant. But constant temperature helps or hurts each species, changing their abundance, age structure, etc., thus altering the competition experienced by each species. When we compare the outcomes with and without temperature variability, we would not know how much of the different is due to temperature variability *per se*, and how much is due to its cascading effects on competitive interactions, age structure, etc. So instead, each term in the invader-resident comparison is evaluated in the situation where all processes are operating, and terms involving $Var(\text{temp})$ quantify the direct effect of variance in temperature. This point can be hard to understand in the abstract, so in our case studies below we highlight where it comes up.

How does fluctuating temperature maintain diatom coexistence?

The most important question about our new approach is, can it tell us something useful? Here we use an empirical case study to argue that it does, by quantifying the mechanisms contributing to coexistence of two diatom species in experiments by Descamps-Julien & Gonzalez (2005). We do this two ways, the first analogous to standard MCT for temporally fluctuating environments, the second based on the trait differences between the species.

Descamps-Julien & Gonzalez (2005) demonstrated that two diatom species, *Cyclotella pseudostelligera* and *Fragilaria crotonensis*, competing for a single limiting resource (silicate), could coexist in a chemostat with periodic variation in temperature, but not at any constant temperature. Ellner *et al.* (2016) showed that the storage effect was not sufficient to explain the diatoms' coexistence and therefore suggested that relative nonlinearity of competition, the only other fluctuation-dependent mechanism in standard MCT, was an essential coexistence mechanism. We were wrong. We forgot about nonlinear averaging of environmental fluctuations, which does not get a stand-alone term in standard MCT, but contributes strongly to coexistence in this community.

Our model, closely following Descamps-Julien & Gonzalez (2005), is a two-species chemostat with some parameters depending on temperature θ,

$$\begin{aligned} \frac{dS}{dt} &= D(S_0 - S) - Q_1(\theta)x_1\frac{V_1(\theta)S}{K_1+S} - Q_2(\theta)x_2\frac{V_2(\theta)S}{K_2+S} \\ \frac{dx_j}{dt} &= x_j\frac{V_j(\theta)S}{K_j+S} - Dx_j, \quad j = 1,2. \end{aligned} \tag{1}$$

Here S is extracellular silicate concentration in the chemostat, x_1 and x_2 are population densities of *Fragilaria* and *Cyclotella*, respectively, S_0 is silicate concentration in the inflow, and D is dilution (outflow) rate. Temperature varies periodically,

$$\theta(t) = \theta_0 + a\sin(2\pi t/P). \tag{2}$$

with mean θ_0, amplitude a, period P. Coexistence was observed experimentally with $\theta_0 = 18°\text{C}$, $a = 6°\text{C}$, $P = 60d$.

Functions specifying how Q_j (silicate per cell) and V_j (maximum cell division rate) depend on temperature were estimated from batch experiments (Fig. 1). As half-saturation constants K_j are nearly constant over the range of temperatures in the experiments (18-24°C), we model them as constant: $K_1 = 0.25\mu$M (*Fragilaria*), $K_2 = 0.14\mu$M (*Cyclotella*). At temperatures of 18°C or lower where both species have similar V values, *Cyclotella* has a significant advantage (smaller K, hence faster nutrient uptake) but at high temperatures *Fragilaria* wins because its V remains high while *Cyclotella*'s falls precipitously.

In the model, species j has silicate- and temperature-dependent instantaneous population growth rate

$$r_j(\theta, S) = \frac{V_j(\theta)S}{K_j + S} - D. \tag{3}$$

Our first analysis begins by partitioning the long-term average population growth rate $\bar{r}$ of each species, in both its invader and resident states, into: the growth rate that would occur without variance in silicate or temperature; the main effects of variance in silicate and in temperature; the interaction between the two variances; and effects of covariance between silicate and temperature.

To do the analysis for species 1, values of $S(t)$ and $\theta(t)$ are recorded from a long simulation of the model with species 1 invading (absent, or kept very rare at all times), and species 2 resident at steady state, using empirically estimated parameters under the experimental conditions. The same analysis could be done with data from a long experiment. Values need to be recorded at times $t_k (k = 1, 2, \cdots, m)$ spaced closely enough to capture all relevant population dynamics, and for long enough to accurately estimate average growth rate; in practice this means that doubling the simulation/experiment duration or doubling the observation frequency has no meaningful effects.

Denote the average values of silicate and temperature across the times t_k by $\overline{S}$ and $\overline{\theta}$, respectively. The average population growth rates of each species are then estimated by time-averaging,

$$\bar{r}_j = \frac{1}{m} \sum_{k=1}^{m} r_j \left(\theta(t_k), S(t_k)\right), \quad j = 1, 2. \tag{4}$$

A population grows if $\bar{r} > 0$.

The growth rate partitioning is depicted in Fig. 2, and formulas for each term are in Table 1. To compute the main effect of silicate variability, for each species define

$$\begin{aligned} \varepsilon_j^0 &= r_j(\bar{\theta}, \bar{S}) \\ \varepsilon_j^S(S) &= r_j(\bar{\theta}, S) - \varepsilon_j^0. \end{aligned} \tag{5}$$

ε_j^0 is the population growth rate with temperature and silicate constant at their means, while ε_j^S is the main effect of silicate concentration varying around its mean, relative to the "null" conditions $(\bar{\theta}, \bar{S})$.[2] Similarly the main effect of temperature variability is

$$\varepsilon_j^\theta(\theta) = r_j(\theta, \bar{S}) - \varepsilon_j^0 \tag{6}$$

The effect of having variability in both S and θ generally will not equal the sum of the main effects. The difference between the actual effect and the sum of main effects is the interaction term,

$$\varepsilon_j^{\theta S}(\theta, S) = r_j(\theta, S) - \left[\varepsilon_j^0 + \varepsilon_j^S + \varepsilon_j^\theta\right]. \tag{7}$$

Re-arranging (7),

$$r_j(\theta, S) = \varepsilon_j^0 + \varepsilon_j^S(S) + \varepsilon_j^\theta(\theta) + \varepsilon_j^{\theta S}(\theta, S). \tag{8}$$

Averaging both sides of (8) as in eqn. (4) gives a partition of average population growth rate into the variance-free growth rate, the main effects of variability in S and in θ, and the interaction between variability in S and in θ:

$$\bar{r}_j = \varepsilon_j^0 + \bar{\varepsilon}_j^S + \bar{\varepsilon}_j^\theta + \bar{\varepsilon}_j^{\theta S}. \tag{9}$$

Following analytic MCT, we further decompose $\bar{\varepsilon}_j^{\theta S}$ into the effect of variance *per se* in θ and S, and the effect of covariance between them. To accomplish this, let $\bar{\varepsilon}_j^{(\theta \# S)}$ denote the expectation of $\varepsilon^{\theta S}$ (eqn. 7) when both have their true univariate distributions but the covariance between them

[2] Means are a natural variance-free null, but other choices are possible, as we explain below.

is removed. And, let $\bar{\varepsilon}_j^{(\theta S)}$ be the effect of restoring the covariance

$$\bar{\varepsilon}_j^{(\theta\#S)} = \bar{\varepsilon}_j^{\theta S} - \bar{\varepsilon}_j^{(\theta S)}. \tag{10}$$

(Ellner *et al.*, 2016) evaluated $\bar{\varepsilon}_j^{(\theta\#S)}$ by temporal randomization to remove correlations; the formulas in Table 1 are the expected value of that process (i.e., the average across infinitely many randomizations). With few main effects the formulas are computationally more efficient, but with many, randomization may be preferable.

Combining eqns. (9) and (10 gives the full decomposition

$$\bar{r}_j = \varepsilon_j^0 + \bar{\varepsilon}_j^S + \bar{\varepsilon}_j^\theta + \bar{\varepsilon}_j^{(\theta\#S)} + \bar{\varepsilon}_j^{(\theta S)}. \tag{11}$$

We call (11) an *E-decomposition* because it decomposes population growth rate into contributions from different aspects of the species' environment.

Next, we compute invader-resident differences by applying the formulas in Table 1 to both species, using $S(t)$ and $\theta(t)$ values from simulations (or experiments) with species 1 invading and species 2 as the resident. Let $\bar{\varepsilon}_{k\backslash j}$ denote a term computed for species k when species j is the invader, and Δ_j the invader-resident difference between corresponding terms when species j is the invader. For example (with $j = 1$ invading, $k = 2$ resident)

$$\Delta_1^S = \bar{\varepsilon}_{1\backslash 1}^S - \bar{\varepsilon}_{2\backslash 1}^S \text{ and } \Delta_1^{(\theta\#S)} = \bar{\varepsilon}_{1\backslash 1}^{(\theta\#S)} - \bar{\varepsilon}_{2\backslash 1}^{(\theta\#S)}. \tag{12}$$

Being a resident at steady state, species 2 has $\bar{r}_2 = 0$. We therefore have

$$\bar{r}_1 = \bar{r}_1 - \bar{r}_2 = \Delta_1^0 + \Delta_1^S + \Delta_1^\theta + \Delta_1^{(\theta\#S)} + \Delta_1^{(\theta S)}. \tag{13}$$

The growth rate $\varepsilon_1^0 = r_1(\bar{\theta}, \bar{S})$ still reflects the temperature fluctuations during the experiment, because the resident's response to temperature affects $\bar{S}$. An alternative, completely fluctuation-independent growth rate is $\varepsilon_1^* = r_1(\bar{\theta}, \bar{S}^*)$, where $\bar{S}^*$ is the mean S in an experiment or simulation at constant temperature $\bar{\theta}$ with species 2 absent. Then $\varepsilon_1^0 = \varepsilon_1^* + \varepsilon_1'$ in (11), where $\varepsilon_1' = \varepsilon_1^0 - \varepsilon_1^*$

is the effect of fluctuation-driven changes in mean S. The term Δ_1^0 in (13) is then replaced by $\Delta_1^* + \Delta_1'$.

Like the analytic formulas in standard MCT, eqn. (13) expresses species 1's invasion growth rate as a sum of contributions from different aspects of the biotic and abiotic environments.[3] Δ_1^0 is the difference in population growth rates at mean temperature and silicate. Δ_1^S is the difference in the main effects of silicate variability, between species 1 as invader and species 2 as resident. This difference results from the nonlinear response of cell division rate to silicate concentration so we call it *relative nonlinearity in silicate*. Similarly, Δ_1^θ measures relative nonlinearity in temperature. We call $\Delta_1^{(\theta S)}$ the storage effect because, as in standard MCT, storage effect is the contribution to population growth rate of covariance between the environment and competitive factors determining r (Ellner *et al.*, 2016).

However, inexact correspondence with MCT is unavoidable. MCT terms such as "storage effect" or "relative nolinearity" refer to terms in small variance approximations that we do not use. Similarly, our variance-interaction terms such as $\bar{\varepsilon}^{(\theta \# S)}$ are absent in standard MCT, because they come from the third- and higher-order terms that are dropped from MCT's Taylor series approximations.

There are also avoidable differences reflecting choices in applying our method. We prefer to decompose in terms of environmental drivers, here temperature and silicate, whereas standard MCT uses an environment-dependent parameter E such as $V(\theta)$, and a competition parameter C, such as the effect of silicate limitation on cell division rate. In sec. SI.3 we present an alternate analysis of this case study using E and C parameters. Also, standard MCT lumps terms that we keep separate. Specifically, the baseline growth rate ($\bar{r}'$ or $\overline{\lambda'}$) in MCT that is described as representing "variation-independent coexistence mechanisms" (Chesson, 2000a, p.224) and "mechanisms operating on a shorter time-scale than the unit of time considered explicitly in the model" (Chesson, 1994, p.249) includes the direct effects of fluctuations in E that are not mediated through variance in C or E, C covariance. Failure to appreciate that led to our incorrect conclusion (Ellner *et al.*, 2016) that relative nonlinearity of competition must be important in this community.

[3] Readers familiar with MCT may ask, where are the scaling factors? We answer that question below, but for this case study it doesn't matter because they are all very near 1 (Ellner *et al.*, 2016).

Results from our E-decomposition are given in Table 2. For each species, the growth rate contributions (Δs) add up (by definition) to equal the invasion growth rates. A negative invasion growth rate would imply that the species could not invade the other. We can therefore assay the importance of each mechanism for coexistence by asking what the invasion growth rate would become if the corresponding contribution is set to zero. The stabilizing component of each mechanism is defined to be its average contribution across species, and the equalizing components are each species' deviation from the average (as in Chesson (2003), but we set the scaling coefficients to 1). Thus, a component is stabilizing (in this sense) simply if its average contribution to the invasion growth rates of all species is positive. [4]

The results in Table 2 show that storage effect, relative nonlinearity in temperature, fluctuation-driven changes in mean silicate, and the fluctuation-free null growth rate are all stabilizing, i.e. they all increase average invasion growth rate. *Cyclotella* has positive invasion growth rate because its fluctuation-free growth rate is large enough to offset the negative contribution from relative nonlinearity in temperature. *Fragilaria*'s positive invasion growth rate is crucially dependent on the positive contribution from relative nonlinearity in temperature, without which its invasion growth rate would become negative. The two largest fluctuation-dependent terms for *Fragilaria* – relative nonlinearity in temperature, and the interaction between temperature and silicate variability – are absent from standard MCT for the reasons explained above.

The E-decomposition identifies how different features of the species' biotic and abiotic environments promote or impede coexistence, given how species respond to their environment. Using the same approach we can additionally do a species-centric decomposition to provide complementary information about which attributes of species promote or impede coexistence under the abiotic and biotic conditions that they experience. We call this a T-decomposition, T standing for "traits."

Given the environment $(S(t), \theta(t))$, population growth rates of *Fragilaria* and *Cyclotella* differ because they have different half-saturation constants K_j (which are constant over the experiment's temperature range) and different temperature-dependent maximum division rates $V_j(\theta)$, which determine their response to silicate concentration. We therefore decompose the invader and

[4]Contrary to intuition, by this definition a mechanism can be stabilizing even if it does not benefit each species when rare. Despite this concern, we follow current usage rather than inventing new terms.

resident population growth rates into the main effects of differences in K and in V, and their interaction, relative to the "null" growth rate that results if both species are given the average responses $\bar{K} = 0.5(K_1 + K_2), \bar{V}(\theta) = 0.5(V_1(\theta) + V_2(\theta))$. Formulas for the terms are in Table 1; we again use Δ to denote a difference between invader and resident terms.

The main effects (Table 3) reiterate the biology: *Cyclotella* benefits from its lower K and is harmed by its lower V at high temperatures, and the reverse is true for *Fragilaria*. Both of these are stabilizing. More unexpected is the size of the interaction terms. Although they are not necessary for coexistence, the invasion growth rates would be quite different without them (nearly an order of magnitude larger for *Cyclotella*).

This T-decomposition could also be applied separately to each component in the E-decomposition, to show which traits generate each growth rate component, but we do not pursue that here.

General Theory

General functional decomposition

The E- and T-decompositions in our diatoms case study (Table 1) are examples of a general *functional decomposition* applicable to any collection of two or more processes, mechanisms, or species differences affecting population growth rate.

The first step is to select the features of interest. A "feature" is some aspect of reality that affects population growth rates. The features in our diatom E-decomposition were variance in S and θ and covariance between them. The features in our diatom T-decomposition were interspecific differences in V and K. In Angert *et al.* (2009) the features were temporal variation in seed germination fraction, temporal variation in seedling growth and survival, and temporal variation in competition. Features in the case studies below include the presence of plant-soil feedbacks, and facilitation of other species by each member of a community.

The decomposition consists of breaking up the long-run growth rate of each species (as invader and then as resident) into (0) a null growth rate in the absence of all selected features; (1) a set of "main effect" terms representing the effect of adding one and only one feature; (2) a set of two-way interaction terms representing the effect of adding each possible pair of features,

above and beyond the sum of their main effects; (3) and so on, until all features are represented. The null term can contribute to coexistence when it includes the stabilizing effects of features that were not selected for the decomposition. Term-by-term invader-resident comparisons then measure the contribution of each growth rate component to invasion growth rates.

In section SI.4 we give a mathematical definition of the decomposition; here we explain it by describing general E- and T-decompositions of population growth rate. We then discuss invader-resident comparisons, and define stabilizing and equalizing components.

General E-decomposition

An E-decomposition follows standard MCT in focusing on coexistence maintained by environmental variability. The features are variances and covariances of biotic or abiotic variables affecting population growth rates. For example, if population growth rate r is a function of environmental variables X, Y, and Z, we write

$$r(X,Y,Z) = \varepsilon^0 + \varepsilon^X + \varepsilon^Y + \varepsilon^Z + \varepsilon^{XY} + \varepsilon^{YZ} + \varepsilon^{XZ} + \varepsilon^{XYZ}. \tag{14}$$

The null growth rate $\varepsilon^0 = r(\overline{X},\overline{Y},\overline{Z})$ is the growth rate when all variables or traits are set to their averages. Terms with superscripts represent the marginal effects of letting all superscripted variables vary while fixing all other variables at their average values — they are the difference between long-run growth with all superscripted variables free, and the sum of all lower-order terms (i.e., terms where fewer variables are free to vary). For example,

$$\begin{aligned}
\varepsilon^X &= r(X,\overline{Y},\overline{Z}) - \varepsilon^0 \\
\varepsilon^{XY} &= r(X,Y,\overline{Z}) - [\varepsilon^X + \varepsilon^Y + \varepsilon^0] \\
\varepsilon^{XYZ} &= r(X,Y,Z) - [\varepsilon^{XY} + \varepsilon^{YZ} + \varepsilon^{XZ} + \varepsilon^X + \varepsilon^Y + \varepsilon^Z + \varepsilon^0].
\end{aligned} \tag{15}$$

Taking expectations of all terms in (14) and (15), each r becomes $\bar{r}$ and each ε becomes $\bar{\varepsilon}$. Mean population growth rate is thus decomposed into the main effects of variation in each argument, and interactions among variation in different arguments.

It is important to recall that each ε only includes the direct effects of variation in superscripted variables; for example $\bar{r}(X, Y, \overline{Z})$ is computed using the distribution of X and Y, and the value of $\overline{Z}$ that occur when Z is fluctuating. Similarly, in a structured population model, presence versus absence of fluctuations in any variable will affect population structures, but terms for the effect of those fluctuations would be evaluated using population growth rates computed with the population structures observed under natural conditions, as in our *Structured populations* example below. If the effect of changes in population structure is a feature of interest, it can be included in the decomposition, producing terms for its main effect, interactions, and so on. *Different decisions about which features are of interest lead to different decompositions.*

Next, we can do a *covariance decomposition* of any $\bar{\varepsilon}$ term with multiple free variables, breaking it up into the effects of their variation *per se* and effects of covariances among them. Our notation convention is that a superscript with parentheses is a term in this secondary decomposition, and a # symbol separate subsets of variables that have within-subset covariation preserved. For example, if r is a function of X, Y, Z, W, and U, then $\bar{\varepsilon}^{(XY\#ZW)}$ is the expectation of r with U set at its average value, X and Y covarying, Z and W covarying, and X and Y independent of Z and W, *minus* all terms with the same nonconstant variables but fewer covariances.

In the diatoms example we had $\bar{\varepsilon}^{XY} = \bar{\varepsilon}^{(X\#Y)} + \bar{\varepsilon}^{(XY)}$. Higher-order terms are broken down similarly with higher-order covariance terms representing the additional affect of the correlations present, beyond the combined effect of all possible lower-order covariance terms. For example,

$$\bar{\varepsilon}^{(XYZ)} = \bar{\varepsilon}^{XYZ} - [\bar{\varepsilon}^{(XY\#Z)} + \bar{\varepsilon}^{(X\#YZ)} + \bar{\varepsilon}^{(XZ\#Y)} + \bar{\varepsilon}^{(X\#Z\#Y)}]. \tag{16}$$

and $\bar{\varepsilon}^{(XY\#Z)}$ is the effect on population growth rate of restoring the observed covariance between X and Y, with Z independent of both, relative to the growth rate when X, Y and Z are mutually independent.

Researchers may wish to decompose only some terms into effects of independent variation and covariation. Alternatively, covariance between two variables could be separated into several components (e.g., rainfall-competition covariance for small individuals and for large individuals), leading to a finer decomposition of the contribution of covariance to population growth.

General T-decomposition

The features in a T-decomposition are attributes that differ among species. The null growth rate is the population growth rate that results from giving all species the across-species average value for each trait; this depends on the scale of measurement, e.g., length versus log length. The main effects are restoring one trait to its true value in all species. Let Θ denote the vector of parameters or variables characterizing the biotic and abiotic environment, possibly time-varying. In the diatoms example, Θ is $(S(t), \theta(t))$ during the experiment. Then if the traits are $X_1, X_2, \cdots, X_n$ the null growth rate is

$$\varepsilon^0 = \mathbb{E}_\Theta\, r(\bar{X}_1, \bar{X}_2, \cdots, \bar{X}_n, \Theta) \tag{17}$$

the hypothetical long-term growth rate when each species has the average value for all traits, but the environment (abiotic and biotic) varying as it actually did with observed traits. The main effect for trait J is

$$\varepsilon^J = \mathbb{E}_\Theta\, r(\bar{X}_1, \cdots, X_J, \cdots, \bar{X}_n, \Theta) - \varepsilon^0. \tag{18}$$

The interaction between traits J and K is

$$\varepsilon^{JK} = \mathbb{E}_\Theta\, r(\bar{X}_1, \cdots, X_J, \cdots, X_K, \cdots, \bar{X}_n, \Theta) - [\varepsilon^J + \varepsilon^K + \varepsilon^0] \tag{19}$$

and so on, exactly as in an E-decomposition. Invader-resident term-by-term differences quantify the contribution of each term to the invading species' advantage when rare. Note, we again measure only the direct effects of each trait by evaluating terms using Θ taken from data or simulations where all traits have their observed values.

Alternatively, the decomposition can include (as additional features) indirect effects mediated by species' effect on their environment. In sect. SI.9.4 we illustrate this alternative, with indirect effects mediated by population structure as the additional feature.

Analogous to covariance decomposition, a step from average to true trait values could be broken into two steps, by considering the intermediate situation where traits vary among species without trait-trait correlations. We do not pursue this refinement because many terms will often be zero (see SI.6.)

Resident weightings in invader-resident comparisons

When comparing invader and resident population growth rates, we generally weight all residents equally. Instead, or additionally, one can ask how an invader gains an advantage over each resident individually. Or, to recover the canonical MCT mechanisms, residents can be weighted by the *scaling factors* q_{ir} (Chesson, 1994, 2000a). These alternative resident weightings are:

$$\begin{aligned}
\Delta_{i,=} &= \bar{\varepsilon}_{i\backslash i} - \frac{1}{\mathcal{S}-1}\sum_{r\neq i}\bar{\varepsilon}_{r\backslash i} && \text{Equal weight} \\
\Delta_{i,k} &= \bar{\varepsilon}_{i\backslash i} - \bar{\varepsilon}_{k\backslash i},\ k \neq i && \text{Pairwise with resident species } k \\
\Delta_{i,q} &= \bar{\varepsilon}_{i\backslash i} - \sum_{r\neq i} q_{ir}\bar{\varepsilon}_{r\backslash i} && \text{Scaling factors}
\end{aligned} \tag{20}$$

where $\mathcal{S}$ is the total number of species. The three weightings are three different but equally valid ways of breaking one number (invasion growth rate of species i) into a sum of interpretable components. The same $\bar{\varepsilon}_{i\backslash i}$ and $\bar{\varepsilon}_{r\backslash i}$ values are used in all weightings, calculated from data or simulations where species i is invading a community with all other species resident. Thus a pairwise comparison between invader A and resident B will include effects of the other residents C, D, E, etc.

In many models the scaling factors q_{ir} do not exist (for example, when there are more limiting factors than species, Barabás *et al.* (2018)). In other cases they are not unique (Ellner *et al.*, 2016), or they can become negative (Snyder *et al.*, 2005, p. E92), turning an invader-resident "difference" into a weighted sum of invader and resident growth rates. Ellner *et al.* (2016) discuss these conceptual difficulties in detail. And in practice, even when well-defined, numerical values of the scaling factors may be very sensitive of choices that should be immaterial in the analytic theory (**?**). Because of these issues, we generally avoid use of the scaling factors.

Stabilizing and equalizing components

We define the *stabilizing* component of any mechanism (i.e., of any Δ term) to be the average of that term across all species as invader. The *equalizing* component of a mechanism is, for each species, its deviation from the average.

Chesson (2000b, 2003) uses similar definitions but first scales population growth rates such that the scaled invasion growth rates sum to zero in the absence of the coexistence mechanisms considered, which eliminates any stabilizing component apart from those mechanisms. While this is aesthetically pleasing, scaling coefficients with this property are only certain to exist when species compete for a single limiting factor (Barabás *et al.*, 2018, sec. 2.7), so we use unscaled population growth rates. The stabilizing component of the null term, if it is nonzero, reflects the stabilizing component of all features not included in the chosen decomposition.

Applications

Spatial coexistence mechanisms in the Chesson (2000) model

To highlight our approach's generality we show how it can be used to analyze coexistence in the Chesson (2000a) model for environments with purely spatial variation. Let $n_{j,x}$ denote abundance of species j in patch $x = 1, 2, \cdots, Q$. The expected contribution of patch x individuals to the global population at time $t+1$ is given by

$$\lambda_j(E_{j,x}(t), C_{j,x}(t)) n_{j,x}(t), \tag{21}$$

where $E_{j,x}$ and $C_{j,x}$ are the environment and competition factors affecting species j in patch x. Apart from space the population is unstructured, so λ_j includes new recruits and survivors. The function λ_j is the same for all patches; intrinsic patch differences are incorporated into $E_{j,x}$ and $C_{j,x}$. For example, $C_{j,x}$ could be population $n_{j,x}$ divided by local carrying capacity $K_{j,x}$.

Chesson (2000a) showed that (with notation as defined in Table 4) the total population of species j has annual growth rate

$$\widetilde{\lambda}_j(t) = \overline{\lambda}_j(t) + Cov_x\left(\nu_j(t), \lambda_j(t)\right), \tag{22}$$

the sum of average patch-specific fitness and fitness-density covariance.

A growing population is represented by $\widetilde{\lambda} > 1$. To parallel the continuous-time case we therefore make the response variable $\widetilde{\lambda} - 1$ as in Chesson (2000a). We can then decompose

$\overline{\lambda}_j(t) - 1$ using the two-factor case of our general E-decomposition. The result is

$$\widetilde{\lambda}_j(t) - 1 = \varepsilon_j^0(t) + \bar{\varepsilon}_j^E(t) + \bar{\varepsilon}_j^C(t) + \bar{\varepsilon}_j^{(E\#C)}(t) + \bar{\varepsilon}_j^{(EC)}(t) + Cov_x(\nu_j(t), \lambda_j(t)). \tag{23}$$

With $\bar{\varepsilon}$ here denoting a spatial average at a particular time. Formulas for all terms are in Table 4.

As in the non-spatial case, mechanism contributions (Δs) are the difference between corresponding $\bar{\varepsilon}$ terms for invader and resident species: e.g. $\Delta_j^C = \bar{\varepsilon}_{j\backslash j}^C - \frac{1}{S-1}\sum_{k\neq j}\bar{\varepsilon}_{k\backslash j}^C$. The invader-resident difference in Cov_x terms is *growth-density covariance* and the difference in $\varepsilon^{(EC)}$ terms corresponds to the *spatial storage effect* as defined by Chesson (2000a). The term Δ^C aligns closely with spatial relative nonlinearity of competition, and Δ^E is spatial relative nonlinearity in environment (absent from the standard decomposition).

Case study: Janzen-Connell effect in grasslands

Petermann *et al.* (2008) developed and parameterized experimentally a spatial model for species coexistence in grasslands through local plant-soil feedbacks mediated by soil microbes. The landscape consists of sites, each containing a single legume, grass, or forb individual, which have a species-specific death rate. Individuals produce seeds each year, which are retained locally (in the parent's site) with probability F (*local retention fraction*), and otherwise disperse at random across all sites. At sites becoming open through death of the occupant, there is lottery competition among seeds, with a twist: a seed's probability of capturing the site depends not only on the identity of the seed and competing seeds, but on the identity of the adult previously occupying the site. Because of persisting species-specific pathogens, a seed is less likely to win a site previously held by a conspecific adult. Specifically, the probability that a seed of type i will capture a site formerly occupied by an adult of type j is $c_{ij}s_i / \sum_k c_{kj}s_k$, where s_k is the number of seeds of type k in a site. Based on experiments, Petermann et al. modeled the soil pathogen effect by assuming $c_{ii} = 0.5$, $c_{i\neq j} = 1$.

In individual-based simulations of the model, Petermann *et al.* (2008) observed long-term coexistence of all species, so long as the local retention fraction F is not too high. To better understand this result in terms of underlying mechanisms, we used a decomposition in which the selected features are the presence of local retention ($F > 0$ vs. $F = 0$) and plant-soil feedback

($c_{ii} = 0.5$ vs. $c_{ii} = 1$). We present here simulation-based results; the decomposition can also be done analytically (sec. SI.8).

Table 4 gives the formulas for decomposing population growth rates; invader-resident comparisons Δ_j used equal weighting of residents. When estimating the $\widetilde{\lambda}_j(t)$ we kept the resident population totals at the steady-state values they assume in the presence of both local seed retention and plant-soil feedbacks (estimated by running a long simulation for each pair of species as residents, with no invader). Each of the $\widetilde{\lambda}_j(t)$ in Table 4 was estimated by repeatedly simulating one time-step forward from those resident densities with the invader occupying one additional site, and averaging over replicates. This ensures that, e.g., Δ^c measures only the direct effects of having or not having plant-soil feedbacks, not the indirect effects mediated by changes in resident species abundance due to presence or absence of plant-soil feedbacks.

Fig. 3 shows the estimated contributions to invasion growth rate of local retention (Δ^F), plant-soil feedbacks (Δ^c), and their interaction, as a function of local retention (F). As expected, local retention in the absence of plant-soil feedbacks (Δ^F) has little effect, but local retention combined with plant-soil feedbacks (Δ^{Fc}) reduces invader growth rates (anti-stabilizing). Plant-soil feedbacks alone (Δ^c) increase the invader growth rate for all species (stabilizing), because in the absence of local retention almost no invader seeds fall into an invader-occupied site, while many resident seeds fall into a site occupied by a conspecific. These results let us understand Petermann et al.'s findings as follows: coexistence occurs when the stabilizing effect of plant-soil feedbacks is not dominated by the anti-stabilizing effect of the interaction between plant-soil feedbacks and local seed retention.

Facilitation and coexistence among beach grasses

Many ecologists have called for coexistence theory to better integrate positive interactions alongside the traditional focus on competition (Bruno *et al.*, 2003; Bulleri *et al.*, 2015; McIntire & Fajardo, 2013). While mechanistic consumer-resource models can readily incorporate positive interactions (Gross, 2008), facilitation in phenomenological, Lotka-Volterra type competition models poses problems for coexistence theory. Positive interspecific interactions (negative competition coefficients, in the Lotka-Volterra convention) can lead to infinite population growth (Gause & Witt, 1935), and additionally Chesson's (2013) expression for niche overlap becomes invalid as can

include the square-root of a negative number. In this section we show how our approach makes it possible to quantify the impacts of positive interactions on coexistence in Lotka-Volterra type models.

Zarnetske *et al.* (2013) used field and experimental data to parameterize a Lotka-Volterra model for beach grass communities in the US Pacific Northwest comprised of *Ammophila arenaria* (AA), *Ammophila breviligulata* (AB), and *Elymus mollis* (EM). Interactions among these species are a mix of competition and facilitation. The Zarnetske *et al.* (2013) model is

$$\frac{dx_i}{dt} = r_i x_i \left(1 - K_i^{-1} \sum_{j=1}^{3} \alpha_{ij} x_j\right) \tag{24}$$

with $\alpha_{ii} = 1$ for $i = 1, 2, 3$. We used parameter estimates from their Table S3-A for low sand input (because those were most robust to the assumed time to reach equilibrium), and the maximum assumed time to equilibrium (because those estimates use the weakest assumptions about unmeasured densities). The estimated competition coefficients are

$$\alpha = \begin{array}{c} \begin{array}{ccc} \text{by AA} & \text{by AB} & \text{by EM} \end{array} \\ \left(\begin{array}{ccc} 1.000 & -0.214 & 0.131 \\ -0.358 & 1.000 & 0.370 \\ 0.089 & -0.139 & 1.000 \end{array}\right) \end{array} \begin{array}{l} \\ \text{on AA} \\ \text{on AB} \\ \text{on EM} \end{array} \tag{25}$$

Negative coefficients indicate facilitation: AA facilitates AB, AB facilitates AA and EM.

We performed a T-decomposition with two main effects, facilitation by AA and facilitation by AB, relative to the no-facilitation situation in which all negative α_{ij} are set to 0. As in the T-decomposition for competing diatoms, we change traits (α values) but leave the environment (equilibrium species abundances) "as is". So for example, paralleling the diatom T-decomposition formulas in Table 1, with species i invading we have

$$\varepsilon_j^0 = r_j \left(1 - K_j^{-1} \sum_{m \neq i} \widetilde{\alpha}_{jm}^0 \bar{x}_m\right), \quad j = 1, 2, 3. \tag{26}$$

where $\bar{x}_m$ is the equilibrium value of x_m when $x_i = 0$ in (24) with the estimated competition coefficients, and $\widetilde{\alpha}^0$ are modified coefficients with facilitation removed by setting all negative values to zero. Because per-capita population growth rates are linear in the competition coefficients, all interaction terms are zero.

Results (Table 5) were calculated for all three resident weightings (eqn. 20). For each species, each column is a partition of the species' invasion growth rate r_{inv} (i.e., each column sums to r_{inv} for the species, apart from rounding errors). For AA and AB the three weightings give equivalent results: facilitation is relatively unimportant, and all species would persist without facilitation because intra-specific competition outweighs inter-specific competition (all resident weightings give identical results for AB, because with AB as a rare invader, neither of the residents AA and EM experiences any direct impacts of facilitation). For EM, the equal weighting and pairwise comparisons are similar: AB facilitation contributes 1/3 to 1/2 of invasion growth rate but is not essential for persistence, while AA facilitation may have a small negative effect. But in the comparison using scaling factors, Δ_q, facilitation by AA makes a large negative contribution. This occurs because $q_{EM,AB} = 4.7$, so facilitation of AB by AA (which is a detriment to EM) is weighted very heavily. The result of this large q_{ir} value is that a feature of low importance in both pairwise comparisons between EM and one resident becomes important when EM is compared to both residents weighted by their scaling factors. Such outcomes are one of our reasons for emphasizing equal-weight and pairwise invader-resident comparisons.

Structured populations: process-specific niche differences in sagebrush steppe

Chu & Adler (2015) used multispecies size-structured integral projection models (IPM) to compare the importance of stabilizing features that act independently on the recruitment (R), survival (S), and growth (G) of the four dominant species in a sagebrush steppe community. Here we revisit their analysis using our approach. The main difference is that the Chu & Adler (2015) analysis was based on invader growth rates, not invader-resident comparisons. See Chu & Adler (2015) for full details of the models, data, and parameter estimation; the main features of the model are summarized in SI.9.

The key model feature for our analysis is that for each demographic rate $V = R, S$ or G there is a matrix α^V of interaction coefficients that determine the impact on that rate of competition

with neighboring plants of each species,

$$\overline{w}_j^V(u,t) = \sum_{k=1}^{4} \alpha_{jk}^V w_{jk}(u,t). \tag{27}$$

Here $w_{jk}(u,t)$ is a measure of average species-k cover within the competition neighborhood of a size-u individual in species j, and $\overline{w}^V(u,t)$ is the overall impact of all neighbors on demographic rate V. Differences between intra- and inter-specific interaction coefficients in α^V generate measures of pairwise "niche difference," defined in SI.9.

We performed a T-decomposition with three main effects, the niche differences affecting recruitment, growth, and survival, represented by the competition coefficients α_{ij}^V. Following Chu & Adler (2015), the "no-niche" state is defined by modifying all between-species α_{ij} values (in α^R, α^S and α^G) so that each pairwise niche overlap ρ_{ij} equals 1, without changing the fitness differences κ_j/κ_i. Formulas for ρ, κ and how they were adjusted are in SI.9. In a two-species Lotka-Volterra community, the values of ρ_{ij} and κ_{ij} determine whether or not all species coexist stably. But with more species, indirect effects can be important (e.g., A facilitates B by harming C). Nonetheless, we regard $\rho_{ij} = 1$ as a reasonable definition of what it means for species i and j to have no niche differences in this model, and Chesson (2013) argued that κ_j/κ_i is a valid general measure of pairwise fitness differences in multispecies communities.

Details of the calculations are in SI.9. The results (Table 6) are qualitatively congruent with the conclusions in Chu & Adler (2015): niche differences affecting recruitment (Δ^R) contribute most to persistence of the grasses, while those affecting survival (Δ^S) are most important for the shrub *Artemisia*. However, one notable difference is that effects of niche differences on growth are detrimental to *Hesperostipa* and *Pseudoroegneria*, and effects on survival are detrimental to *Pseudoroegneria*, whereas (Chu & Adler, 2015, Fig. 5C) concluded that all effects of niche differences are at least mildly helpful. The detrimental effects arise in our analysis because benefits to an invading grass species are outweighed by larger benefits to their competitor *Artemisia*. When our analysis is re-done with *Artemisia* removed from the community (results not shown), all effects of niche differences are helpful to all three grasses. This difference between our analysis and Chu & Adler (2015) illustrates the importance of invader-resident comparison: a seemingly beneficial feature may hurt you by helping your competitor more than it helps you.

Discussion

We believe that the mathematical complexity and subtleties of standard MCT, and the approximate analytic formulas it requires for empirical applications, have obscured the simplicity, generality, and power of the underlying ideas, and obstructed the path to empirical applications. We have tried to break this logjam by separating the underlying concepts from the mathematical implementation, and providing a more general computational implementation. Our approach is not a replacement for analytic MCT – it is an additional tool, for detailed analysis of specific systems.

We abandon analytic MCT's requirement to use scaling factors q_{ir} in invader-resident growth rate comparisons. The scaling factors remove a term from the analytic growth rate decompositions for fluctuation-dependent mechanisms, allowing some necessary calculations even when the dynamics of the limiting factors for which species compete are unknown (Barabás *et al.*, 2018). That term is not problematic in our approach, because all terms are evaluated using experimental or simulated data. Similarly, we abandon growth rate scalings in stablizing components, which have a firm theoretical foundation only for the case of a single limiting factor (Barabás *et al.*, 2018)). We also do not use the small-variance approximations that eliminate many interaction terms.

The main benefit of our approach is that analytic formulas are replaced by simulations or data, so new case studies or coexistence mechanisms do not require new math. This benefit is illustrated by our case studies, which include features (higher-order interactions between temperature and resource variability, interacting fluctuation-independent spatial mechanisms, facilitation, and stage-specific niche differences in structured populations) that have not been analyzed within the standard framework. Many of these probably could be analyzed in the standard framework, given enough time, but our approach gives more accurate and more complete answers, with much less effort.

The main weakness of our approach is that analytic formulas are replaced by simulations or data, so we do not get the generality and qualitative insights that can come from analytic formulas for coexistence mechanisms. Levins (1966) contrasted three incompatible goals of population modeling: generality, realism, and precision. Our approach provides realism and precision,

giving a complete decomposition when the processes in a community have been modeled quantitatively, but the results are specific to the modeled community. Generality, a strength of analytic MCT, can only emerge with our approach by identifying general patterns in numerical results.

Like analytic MCT, our approach requires a way to calculate population growth rates as a function of the factors that determine their values at any time, and data (empirical, or simulation-derived) on the patterns of variation in those factors. There is no methodological cure for this requirement. To fully understand how species coexist we need to know what factors limit population growth rates, and quantify the impacts of each factor. Measuring and modeling population responses to multiple limiting factors in the field is especially challenging for long-lived species with complex life cycles, but even for short-lived species such as annual plants, describing population responses to variation in community composition and spatial and temporal environmental variation can be difficult. However, like analytic MCT our approach can also be applied to a single component of population growth rate, in the manner of Sears & Chesson (2007) who compared the contributions of spatial storage effect and local resource competition to seed yield in two desert annuals. This is accomplished by using the focal component (e.g., per capita fecundity) as the response variable, rather than population growth rate, and empirical data on the driving variables.

Discussion about how to quantify coexistence mechanisms will benefit from applying our approach to more case studies. Several times a new case study revealed to us that a seemingly wonderful idea was fatally flawed. Abandoning the scaling factors q_{ir} may be contentious, and therefore is likely to evolve. We have noted conceptual and practical difficulties with the q_{ir}, and suggested equal weighting of residents as a simple alternative, but equal weighting may not be appropriate when some resident species are far more common than others. Our approach also needs to be expanded further to encompass many important situations that we cannot yet address, including spatiotemporal variation, many individual- or grid-based spatial models (e.g., Adler *et al.*, 2006), and processes occurring continuously in time as organisms move through space.

Acknowledgments We thank our pre-submission and anonymous reviewers for comments and insightful questions that led to new analyses, substantial restructuring and a more user-friendly paper. We thank the authors of Barabás *et al.* (2018) for sharing their paper prior to publication and for discussions that deepened our understanding of MCT. This research was supported by US NSF grants DEB 1353039 (SPE and GJH), DEB 1354041 (RES), and DEB 1353078 (PBA).

Literature Cited

Abu Baker, M.A. & Brown, J.S. (2014). Foraging in space and time structure an African small mammal community. *Oecologia*, 175, 521–535.

Adler, P.B., Ellner, S.P. & Levine, J.M. (2010). Coexistence of perennial plants: an embarrassment of niches. *Ecology Letters*, 13, 1019–1029.

Adler, P.B., HilleRisLambers, J., Kyriakidis, P., Guan, Q. & Levine, J.M. (2006). Climate variability has a stabilizing effect on coexistence of prairie grasses. *Proc. Nat. Acad. Sci. U. S. A.*, 103, 12793–12798.

Angert, A.L., Huxman, T.E., Chesson, P. & Venable, D.L. (2009). Functional tradeoffs determine species coexistence via the storage effect. *Proceedings of the National Academy of Sciences (USA)*, 106, 11641 – 11645.

Bagchi, R., Gallery, R.E., Gripenberg, S., Gurr, S.J., Narayan, L., Addis, C.E., Freckleton, R.P. & Lewis, O.T. (2014). Pathogens and insect herbivores drive rainforest plant diversity and composition. *Nature*, 506, 85–88.

Barabás, G., D'Andrea, R. & Stump, S.M. (2018). Chesson's coexistence theory. *Ecological Monographs*, 88, 277 – 303.

Brown, J. (1989). Desert rodent community structure - a test of 4 mechanisms of coexistence. *Ecological Monographs*, 59, 1–20.

Bruno, J.F., Stachowicz, J.J. & Bertness, M.D. (2003). Inclusion of facilitation into ecological theory. *Trends in Ecology and Evolution*, 18, 119–125.

Bulleri, F., Bruno, J.F., Silliman, B.R., Stachowicz, J.J. & Michalet, R. (2015). Facilitation and the niche: implications for coexistence, range shifts and ecosystem functioning. *Functional Ecology*, 30, 70–78.

Caley, M. (1995). Reef-fish community structure and dynamics: An interaction between local and larger-scale processes? *Marine Ecology Progress Series*, 129, 19–29.

Chesson, P. (1994). Multispecies competition in variable environments. *Theoretical Population Biology*, 45, 227–276.

Chesson, P. (2000a). General theory of competitive coexistence in spatially-varying environments. *Theoretical Population Biology*, 58, 211–237.

Chesson, P. (2000b). Mechanisms of maintenance of species diversity. *Annual Review of Ecology and Systematics*, pp. 343–366.

Chesson, P. (2003). Quantifying and testing coexistence mechanisms arising from recruitment fluctuations. *Theoretical Population Biology*, 64, 345 – 357.

Chesson, P. (2011). Ecological niches and diversity maintenance. In: *Research in Biodiversity — Models and Applications* (ed. Pavlinov, I.Y.). InTech, Rijeka, Croatia, pp. 43–60.

Chesson, P. (2013). Species competition and predation. In: *Ecological Systems: Selected Entries from the Encyclopedia of Sustainability Science and Technology* (ed. Leemans, R.). Springer, chap. 13, pp. 223–256.

Chu, C. & Adler, P.B. (2015). Large niche differences emerge at the recruitment stage to stabilize grassland coexistence. *Ecological Monographs*, 85, 373 – 392.

Comita, L.S., Queenborough, S.A., Murphy, S.J., Eck, J.L., Xu, K., Krishnadas, M., Beckman, N. & Zhu, Y. (2014). Testing predictions of the JanzenConnell hypothesis: a meta-analysis of experimental evidence for distance- and density-dependent seed and seedling survival. *Journal of Ecology*, 102, 845–856.

Descamps-Julien, B. & Gonzalez, A. (2005). Stable coexistence in a fluctuating environment: an experimental demonstration. *Ecology*, 86, 2815 – 2824.

Dybzinski, R. & Tilman, D. (2007). Resource use patterns predict long-term outcomes of plant competition for nutrients and light. *American Naturalist*, 170, 305–318.

Ellner, S.P., Snyder, R.E. & Adler, P.B. (2016). How to quantify the temporal storage effect using simulations instead of math. *Ecology Letters*, 19, 1333–1342.

Gause, G.F. & Witt, A.A. (1935). Behavior of Mixed Populations and the Problem of Natural Selection. *The American Naturalist*, 69, 596–609.

Godoy, O. & Levine, J.M. (2014). Phenology effects on invasion success: insights from coupling field experiments to coexistence theory. *Ecology*, 95, 726–736.

Gross, K. (2008). Positive interactions among competitors can produce species-rich communities. *Ecology Letters*, 11, 929–936.

Grubb, P.J. (1977). The maintenance of species-richness in plant communities: the importance of the regeneration niche. *Biological Rev*, 52, 107 – 145.

Holt, R.D. & Bonsall, M.B. (2017). Apparent competition. *Annual Review of Ecology, Evolution, and Systematics*, 48, 447–471.

Hubbell, S.P. (2001). *The Unified Neutral Theory of Biodiversity and Biogeography*. Princeton University Press, Princeton, N.J.

Hutchinson, G. (1961). The paradox of the plankton. *American Naturalist*, 95, 137 – 145.

Hutchinson, G.E. (1959). Homage to santa rosalia or why are there so many kinds of animals? *The American Naturalist*, 93, 145–159.

Kotler, B. & Brown, J. (1988). Environmental heterogeneity and the coexistence of desert rodents. *Annual Review of Ecology and Systematics*, 19, 281–307.

Letten, A.D., Dhami, M.K., Ke, P.J. & Fukami, T. (2018). Species coexistence through simultaneous fluctuation-dependent mechanisms. *Proceedings of the National Academy of Sciences*.

Levins, R. (1966). The strategy of model building in population ecology. *American Scientist*, 54, 421 – 431.

Lönnberg, K. & Eriksson, O. (2013). Rules of the seed size game: contests between large-seeded and small-seeded species. *Oikos*, 122, 1080–1084.

McIntire, E.J.B. & Fajardo, A. (2013). Facilitation as a ubiquitous driver of biodiversity. *New Phytologist*, 201, 403–416.

Metcalf, C.J.E., Ellner, S.P., Childs, D.Z., Salguero-Gómez, R., Merow, C., McMahon, S.M., Jongejans, E. & Rees, M. (2015). Statistical modelling of annual variation for inference on stochastic population dynamics using Integral Projection Models. *Methods in Ecology and Evolution*, 6, 1007–1017.

Munday, P. (2004). Competitive coexistence of coral-dwelling fishes: The lottery hypothesis revisited. *Ecology*, 85, 623–628.

Petermann, J.S., Fergus, A.J.F., Turnbull, L.A. & Schmid, B. (2008). Janzen-Connell effects are widespread and strong enough to maintain diversity in grasslands. *Ecology*, 89, 2399–2406.

Sale, P. (1979). Recruitment, loss and coexistence in a guild of territorial coral-reef fishes. *Oecologia*, 42, 159–177.

Sears, A.L.W. & Chesson, P. (2007). New methods for quantifying the spatial storage effect: an illustration with desert annuals. *Ecology*, 88, 2240–2247.

Shmida, A. & Ellner, S. (1984). Coexistence of plant species with similar niches. *Vegetatio*, 58, 29–55.

Silvertown, J., Dodd, M., Gowing, D. & Mountford, J. (1999). Hydrologically defined niches reveal a basis for species richness in plant communities. *Nature*, 400, 61–63.

Snyder, R.E., Borer, E.T. & Chesson, P. (2005). Examining the relative importance of spatial and nonspatial coexistence mechanisms. *The American Naturalist*, 166, E75 – E94.

Usinowicz, J., Chang-Yang, C.H., Chen, Y.Y., Clark, J.S., Fletcher, C., Garwood, N.C., Hao, Z., Johnstone, J., Lin, Y., Metz, M.R., Masaki, T., Nakashizuka, T., Sun, I.F., Valencia, R., Wang, Y., Zimmerman, J.K., Ives, A.R. & Wright, S.J. (2017). Temporal coexistence mechanisms contribute to the latitudinal gradient in forest diversity. *Nature*, 550, 105–108.

Volkov, I., Banavar, J.R., Hubbell, S.P. & Maritan, A. (2007). Patterns of relative species abundance in rainforests and coral reefs. *Nature*, 450, 45–49.

Zarnetske, P.L., Gouhier, T.C., Hacker, S.D., Seabloom, E.W. & Bokil, V.A. (2013). Indirect effects and facilitation among native and non-native species promote invasion success along an environmental stress gradient. *Journal of Ecology*, 101, 905 – 915.

Ziv, Y., Abramsky, Z., Kotler, B. & Subach, A. (1993). Interference competition and temporal and habitat partitioning in 2 gerbil species. *Oikos*, 66, 237 – 246.

Table 1: Calculation formulas for the diatoms case study

Term	Formula	Meaning
$\bar{\theta}$	$\frac{1}{m}\sum_{k=1}^{m}\theta(t_k)$	Mean temperature
$\bar{S}$	$\frac{1}{m}\sum_{k=1}^{m}S(t_k)$	Mean silicate, varying temperature experiment or simulation
$\overline{S^*}$	$\frac{1}{m}\sum_{k=1}^{m}S^*(t_k)$	Mean silicate, constant temperature experiment or simulation
$\varepsilon_j^0,\ \varepsilon_j^*$	$r_j(\bar{S},\bar{\theta}),\ r_j(\overline{S^*},\bar{\theta})$	Population growth rates at mean temperature and silicate
ε_j'	$\varepsilon_j^0-\varepsilon_j^*$	Effect of fluctuation-driven change in mean S
$\bar{\varepsilon}_j^S$	$\frac{1}{m}\sum_{k=1}^{m}r_j\left(\bar{\theta},S(t_k)\right)-\varepsilon_j^0$	Main effect of variation in silicate
$\bar{\varepsilon}_j^\theta$	$\frac{1}{m}\sum_{k=1}^{m}r_j\left(\theta(t_k),\bar{S}\right)-\varepsilon_j^0$	Main effect of variation in temperature
$\bar{\varepsilon}_j^{\theta S}$	$\frac{1}{m}\sum_{k=1}^{m}r_j\left(\theta(t_k),S(t_k)\right)-\left[\varepsilon_j^0+\bar{\varepsilon}_j^S+\bar{\varepsilon}_j^\theta\right]$	Interaction of silicate and temperature variation
$\bar{\varepsilon}_j^{(\theta\#S)}$	$\frac{1}{m^2}\sum_{k=1}^{m}\sum_{i=1}^{m}r_j\left(\theta(t_k),S(t_i)\right)-\left[\varepsilon_j^0+\bar{\varepsilon}_j^S+\bar{\varepsilon}_j^\theta\right]$	Independent variation component of $\bar{\varepsilon}_j^{\theta S}$
$\bar{\varepsilon}_j^{(\theta S)}$	$\bar{\varepsilon}_j^{\theta S}-\bar{\varepsilon}_j^{(\theta\#S)}$	Covariance component of $\bar{\varepsilon}_j^{\theta S}$
$r(V,K,S)$	$\frac{VS}{K+S}-D$	Instantaneous population growth rate as a function of traits and silicate concentration
ε_j^0	$\frac{1}{m}\sum_{k=1}^{m}r(\overline{V}(\theta(t_k)),\overline{K},S(t_k))$	Baseline (equal-traits) mean population growth rate
$\bar{\varepsilon}_j^V$	$\frac{1}{m}\sum_{k=1}^{m}r(V_j(\theta(t_k)),\overline{K},S(t_k))-\varepsilon_j^0$	Main effect of differences in $V(\theta)$
$\bar{\varepsilon}_j^K$	$\frac{1}{m}\sum_{k=1}^{m}r(\overline{V}(\theta(t_k)),K_j,S(t_k))-\varepsilon_j^0$	Main effect of differences in $K(\theta)$
$\bar{\varepsilon}_j^{VK}$	$\frac{1}{m}\sum_{k=1}^{m}r(V_j(\theta(t_k)),K_j,S(t_k))-\left[\varepsilon_j^0+\bar{\varepsilon}_j^V+\bar{\varepsilon}_j^K\right]$	Interaction of V and K differences

$S(t_k)$ are values from a model run or experiment with time-varying temperature, $S^*(t_k)$ from a run or experiment with constant temperature $\bar{\theta}$. In these experiments $S^*(t_k)$ is constant so there is no need to time-average, but in other experiments that might not be true so we give the general formulas. j is the species index in all formulas. Formulas above the dashed line are the environment-centric E decomposition; formulas below the dashed line are the trait-centered T decomposition. To compute the invasion growth rate components Δ_i for species i, the formulas are applied to both species ($j = 1, 2$) using data

or model simulations with species j as the invader and the other species resident, and each Δ_j is the difference between corresponding $\bar{\varepsilon}_j$ for the invader and the resident.

Table 2: E-decomposition of coexistence mechanisms for experiments with two diatom species (Descamps-Julien & Gonzalez, 2005).

Growth rate contributions	*Fragilaria* $r_{inv} = 0.061$ d^{-1}	*Cyclotella* $r_{inv} = 0.007$ d^{-1}	Stabilizing component
Fluctuation-free growth rate, Δ^*	-0.031	0.041	0.005
Fluctuation-driven change in mean S, Δ'	0.020	0.001	0.011
Relative nonlinearity in temperature θ, Δ^{θ}	0.092	-0.037	0.028
Relative nonlinearity in silicate S, Δ^{S}	-0.014	-0.001	-0.007
θ, S variance interaction, $\Delta^{(\theta \# S)}$	-0.045	0.000	-0.022
θ, S covariance (storage effect), $\Delta^{(\theta S)}$	0.038	0.003	0.021

Values were calculated from the last 1200 days of a 3600 day simulation, recording 10 values each day. Growth rate contributions (Δ) are invader-resident pairwise differences in the decompositions of invader and resident growth rates; for each species, the sum of all Δs equals the invasion growth rate r_{inv}. Recall that $\Delta^* + \Delta' = \Delta^0$, as explained following eqn. (13). The stabilizing component of each is simply the average of the first two numerical columns; equalizing components (not tabulated) are the deviations between each species' Δ and that average. The storage effect estimates here differ slightly from Ellner *et al.* (2016) because here we are not using the scaling factors in invader-resident comparisons. Values calculated by `ForcedChemo_Func_Covar.R`, and `ForcedChemoSubs.R`

Table 3: T-decomposition of coexistence mechanisms for experiments with two diatom species (Descamps-Julien & Gonzalez, 2005), using the formulas in Table 1.

Growth rate contributions	*Fragilaria* $r_{inv} = 0.061$ d^{-1}	*Cyclotella* $r_{inv} = 0.007$ d^{-1}	Stabilizing component
Difference in K, Δ^K	-0.057	0.079	0.011
Difference in V, Δ^V	0.079	-0.017	0.031
Interaction, Δ^{VK}	0.039	-0.054	-0.007

All species necessarily have the same null growth rate so the corresponding invader-resident comparison Δ^0 is zero. The stabilizing component of each growth rate contribution is the average of the first two numerical columns; equalizing components (not tabulated) are the deviations between each species' Δ and that average. Tabulated values are calculated in `ForcedChemo_TraitDecomp.R` and `ForcedChemoSubs.R`.

Table 4: Calculation formulas for analysis of spatial coexistence mechanisms.

Term	Formula	Meaning
$\overline{N}_j(t)$	$Q^{-1}\sum_{x=1}^{Q} n_{j,x}(t)$	Average within-patch abundance
$\nu_{j,x}(t)$	$n_{j,x}(t)/\overline{N}_j(t)$	Relative abundance in patch x
$\lambda_{j,x}(t)$	$\lambda_j(E_{j,x}(t), C_{j,x}(t))$	Per-capita fitness of patch x individuals
$\bar{\nu}_j(t),\ \bar{\lambda}_j(t)$	$Q^{-1}\sum_{x=1}^{Q} \nu_{j,x}(t),\ Q^{-1}\sum_{x=1}^{Q} \lambda_{j,x}(t)$	Spatial averages of ν, λ
$\overline{E}_j(t),\ \overline{C}_j(t)$	$Q^{-1}\sum_{x=1}^{Q} E_{j,x}(t),\ Q^{-1}\sum_{x=1}^{Q} C_{j,x}(t)$	Average environment and competition factors
$Cov_x(\nu_j(t), \lambda_j(t))$	$\left[Q^{-1}\sum_{x=1}^{Q} \nu_{j,x}(t)\lambda_{j,x}(t))\right] - \bar{\nu}_j(t)\bar{\lambda}_j(t)$	Fitness-density covariance
$\varepsilon_j^0(t)$	$\lambda_j(\overline{E}_j(t), \overline{C}_j(t)) - 1$	Baseline (zero variance) population growth rate
$\bar{\varepsilon}_j^C(t)$	$[Q^{-1}\sum_{x=1}^{Q} \lambda_j(\overline{E}_j(t), C_{j,x}(t)) - 1] - \varepsilon_j^0(t)$	Main effect of spatial variance in C
$\bar{\varepsilon}_j^E(t)$	$[Q^{-1}\sum_{x=1}^{Q} \lambda_j(E_{j,x}(t), \overline{C}_j(t)) - 1] - \varepsilon_j^0(t)$	Main effect of spatial variance in E
$\bar{\varepsilon}_j^{EC}$	$[\bar{\lambda}_j(t) - 1] - \left[\varepsilon_j^0 + \bar{\varepsilon}_j^E + \bar{\varepsilon}_j^C\right]$	Interaction of E and C variation
$\bar{\varepsilon}_j^{(E\#C)}$	$\left[Q^{-2}\sum_{x=1}^{Q}\sum_{y=1}^{Q} \lambda_j(E_{j,x}(t), C_{j,y}(t)) - 1\right] - \left[\varepsilon_j^0 + \bar{\varepsilon}_j^E + \bar{\varepsilon}_j^C\right]$	Independent variation component of $\bar{\varepsilon}_j^{EC}$
$\bar{\varepsilon}_j^{(EC)}$	$\bar{\varepsilon}_j^{EC} - \bar{\varepsilon}_j^{(E\#C)}$	Covariance variance component of $\bar{\varepsilon}_j^{EC}$
$\widetilde{\lambda}_j(t)$	(total pop. at $t+1$)/(total pop. at t)	Population growth rate
$\bar{\varepsilon}_j^0(t)$	$\widetilde{\lambda}_j(F = 0, c_{ii} = 1)(t) - 1$	Baseline growth rate
$\bar{\varepsilon}_j^c(t)$	$[\widetilde{\lambda}_j(F = 0, c_{ii} = 0.5)(t) - 1] - \varepsilon_j^0(t)$	Main effect of plant-soil feedbacks c
$\bar{\varepsilon}_j^F(t)$	$[\widetilde{\lambda}_j(F \neq 0, c_{ii} = 1)(t) - 1] - \varepsilon_j^0(t)$	Main effect of local retention F
$\bar{\varepsilon}_j^{Fc}(t)$	$[\widetilde{\lambda}_j(F \neq 0, c_{ii} = 0.5)(t) - 1] - [\varepsilon_j^c(t) + \bar{\varepsilon}_j^F(t) + \bar{\varepsilon}_j^0(t)]$	Interaction of c and F

j is the species index in all formulas. Formulas above the dashed line are a spatial E-decomposition for the Chesson (2000a) model with purely spatial variation. Formulas below the dashed line are a T-decomposition for the Petermann *et al.* (2008) model. The argument $c_{ii} = 1$ means that all entries of c equal 1 (no plant-soil feedbacks), while $c_{ii} = 0.5$ means that all diagonal entries of c equal 0.5 (negative plant-soil feedbacks). Similarly, F is either zero for all species (no local retention) or has the same positive value for all species. Formulas for the various $\widetilde{\lambda}_j(t)$ are given in sec. SI.8.

All formulas here are for spatial "snapshot" data at one time t, or one observation of population growth. If data at multiple times are available, each ε or $\bar{\varepsilon}$ term is calculated for each time point, then averaged over time.

Table 5: Results for the beach grass model of Zarnetske *et al.* (2013) with different resident weightings.

	Ammophila arenaria (AA) $\bar{r}_{inv} = 0.17$/month				*Ammophila breviligulata* (AB) $\bar{r}_{inv} = 0.25$/month				*Elymus mollis* (EM) $\bar{r}_{inv} = 0.36$/month			
	Equal	q_{ir}	$-$AB	$-$EM	Equal	q_{ir}	$-$AA	$-$EM	Equal	q_{ir}	$-$AA	$-$AB
Δ^0	0.19	0.14	0.14	0.25	0.19	0.19	0.19	0.19	0.24	0.62	0.23	0.26
Δ^{AA}	0.00	0.00	0.00	0.00	0.06	0.06	0.06	0.06	-0.04	-0.38	0.00	-0.08
Δ^{AB}	-0.02	0.03	0.03	-0.08	0.00	0.00	0.00	0.00	0.15	0.11	0.12	0.18

Growth rate contribution Δ^0 is invader-resident comparison of "null" growth rates when all facilitation is eliminated, and Δ^{AA} and Δ^{AB} are the main effects of facilitation by AA and AB, respectively. The different invader-resident weightings (column headings) are defined in eqn. (20); "Equal" denotes equal weighting of residents, q_{ir} denotes weighting by Chesson's scaling factors, and "$-$XY" denotes a pairwise comparison between the species in the table heading as the invader, with competing species XY as resident. The scaling factors q_{ir} are derived in sect. SI.7. Tabulated values are calculated by `Beachgrass_TraitDecomp.R` and `BeachgrassFuns.R`

Table 6: Main effects and interactions of niche differences impacting *R*ecruitment, *G*rowth, and *S*urvival in the four dominant species in Idaho sagebrush steppe.

Species	$\bar{r}_{inv}$ (1/yr)	Δ^0	Δ^R	Δ^G	Δ^S	Δ^{RG}	Δ^{RS}	Δ^{GS}	Δ^{RGS}
Artemisia tripartita	0.015	-1.16	0.00	0.55	0.68	-0.01	-0.02	-0.03	0.01
Hesperostipa comata	0.25	0.12	0.13	-0.06	0.09	-0.01	-0.03	0.01	0.00
Poa secunda	0.43	0.15	0.29	0.03	0.04	-0.04	-0.06	0.00	0.01
Pseudoroegneria spicata	0.20	0.35	0.10	-0.20	-0.04	-0.00	-0.01	0.01	0.00
Stabilizing			0.13	0.08	0.19	-0.02	-0.03	-0.00	0.01

$\bar{r}_{inv}$ is invasion growth rate when niche differences at all stages are present, and Δ_0 is the no-niche-differences growth rate. Tabulated values were calculated by `partition_simulations.R` and scripts that it sources.

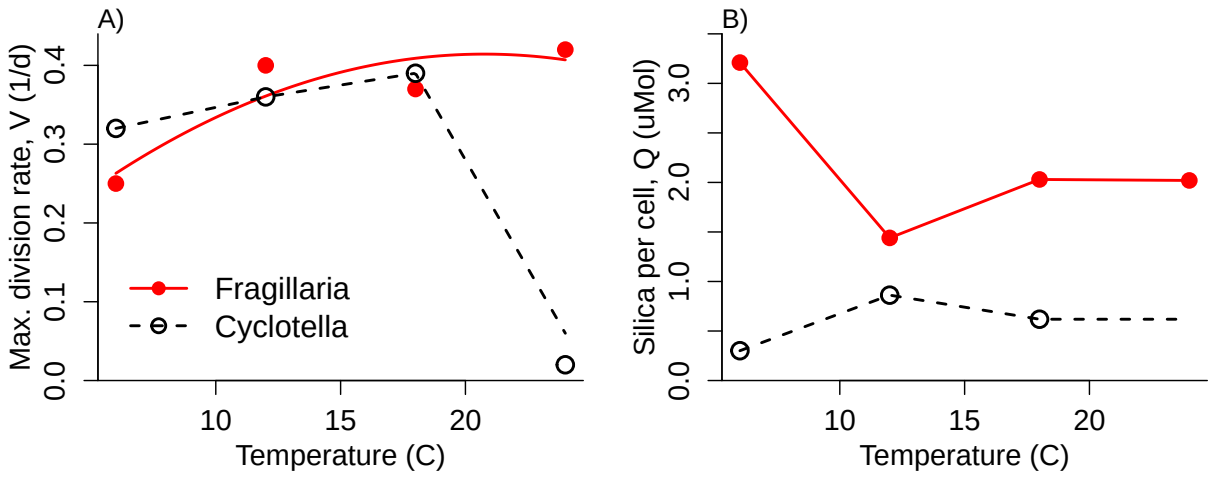

Figure 1: Species-specific temperature responses of the parameters A) V, and B) Q, governing nutrient uptake and conversion efficiency. Points (closed circles: *Fragilaria*, open circles: *Cyclotella*) are parameter estimates derived from 9-day single-species batch experiments on each species at a constant temperature (Table 1 of Descamps-Julien & Gonzalez (2005)). The plotted lines and curves were used to simulate the model with continuously varying temperature. Q for *Cyclotella* could not be estimated at 24°C because of its very low growth rate in the batch experiments. Because *Cyclotella*'s growth at 24°C was much better in chemostats than in batch experiments, our V function for *Cyclotella* (dashed line in panel A) uses a higher value of V at 24°C, chosen so that the model matches better the average abundance of *Cyclotella* in chemostat experiments; but even without this modification the model predicts coexistence in the variable temperature experiment. Figure generated by `PlotForcedChemo.R, ForcedChemoSubs.R`

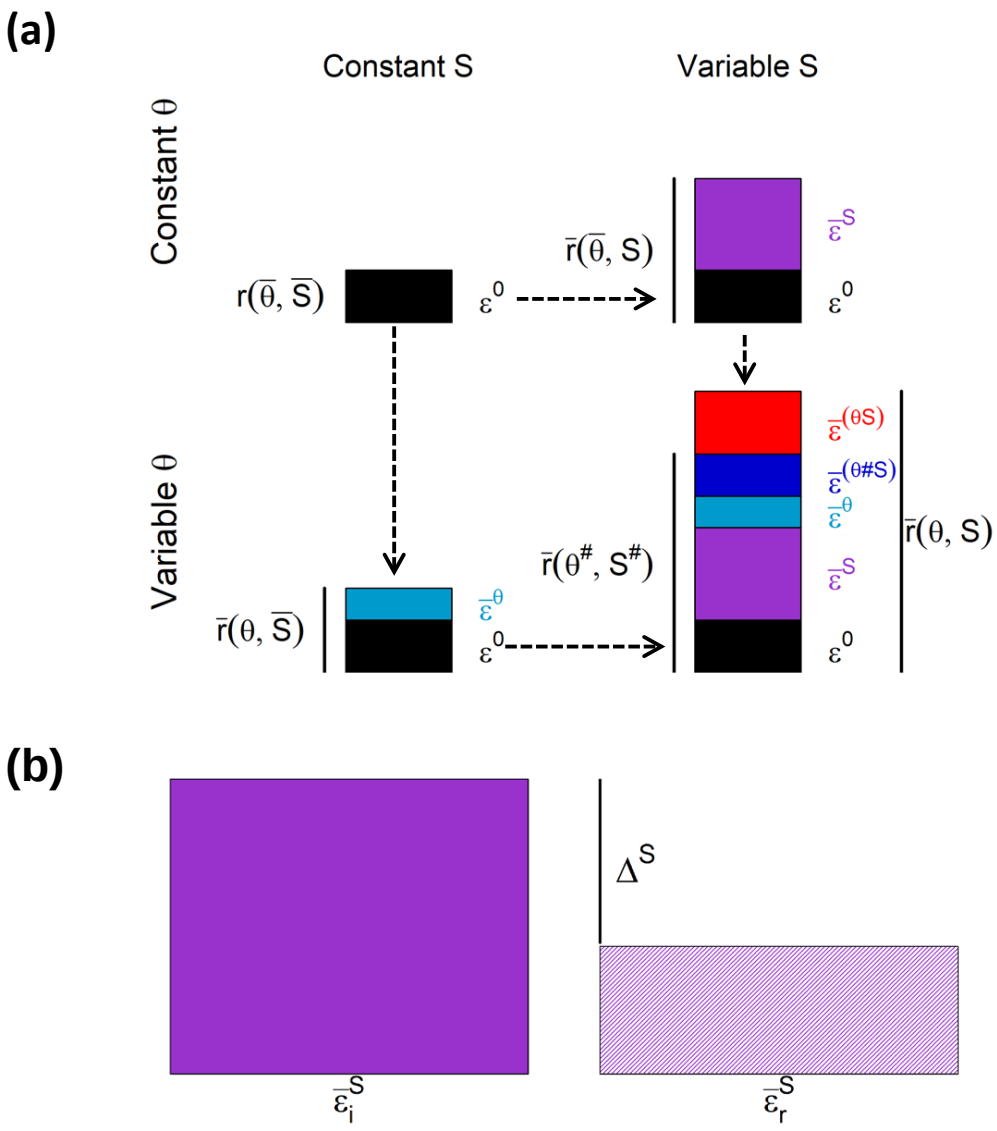

Figure 2: (a) Conceptual representation of how population growth rate is partitioned for any one species, as invader or resident, in the diatoms case study. ε^0 (black, top left) is growth rate when temperature θ and silicate S are held constant at their average values. $\bar{\varepsilon}^S$ (purple, top right) is the change in growth rate $\bar{r}$ when silicate varies but temperature remains constant at its average value, and $\bar{\varepsilon}^\theta$ (cyan, bottom left) is the change in growth rate when temperature varies but silicate remains constant at its average value. The further change in growth rate when both vary (bottom right), beyond the combined effect of each varying on its own, is partitioned into the effect of uncorrelated joint variation $\bar{\varepsilon}^{(\theta\#S)}$ (dark blue) and the additional effect of correlations between silicate and temperature $\bar{\varepsilon}^{(\theta S)}$ (red); $\bar{r}(\theta^\#, S^\#)$ is the long-run growth rate when θ and S vary in an uncorrelated way, given by the first term in the formula for $\bar{\varepsilon}_j^{(\theta\#S)}$ in Table 1. For clarity, this figure is drawn for a hypothetical case where all terms in the partitioning are positive. (b) Conceptual representation of how a term-by-term comparison of invader species i and resident species r defines the contribution Δ of a coexistence mechanism to invader growth rate. This illustrates the case where there is only one resident species. Figure generated by `AwesomeSchematic.R` and `AwesomeSchematicPart2.R`

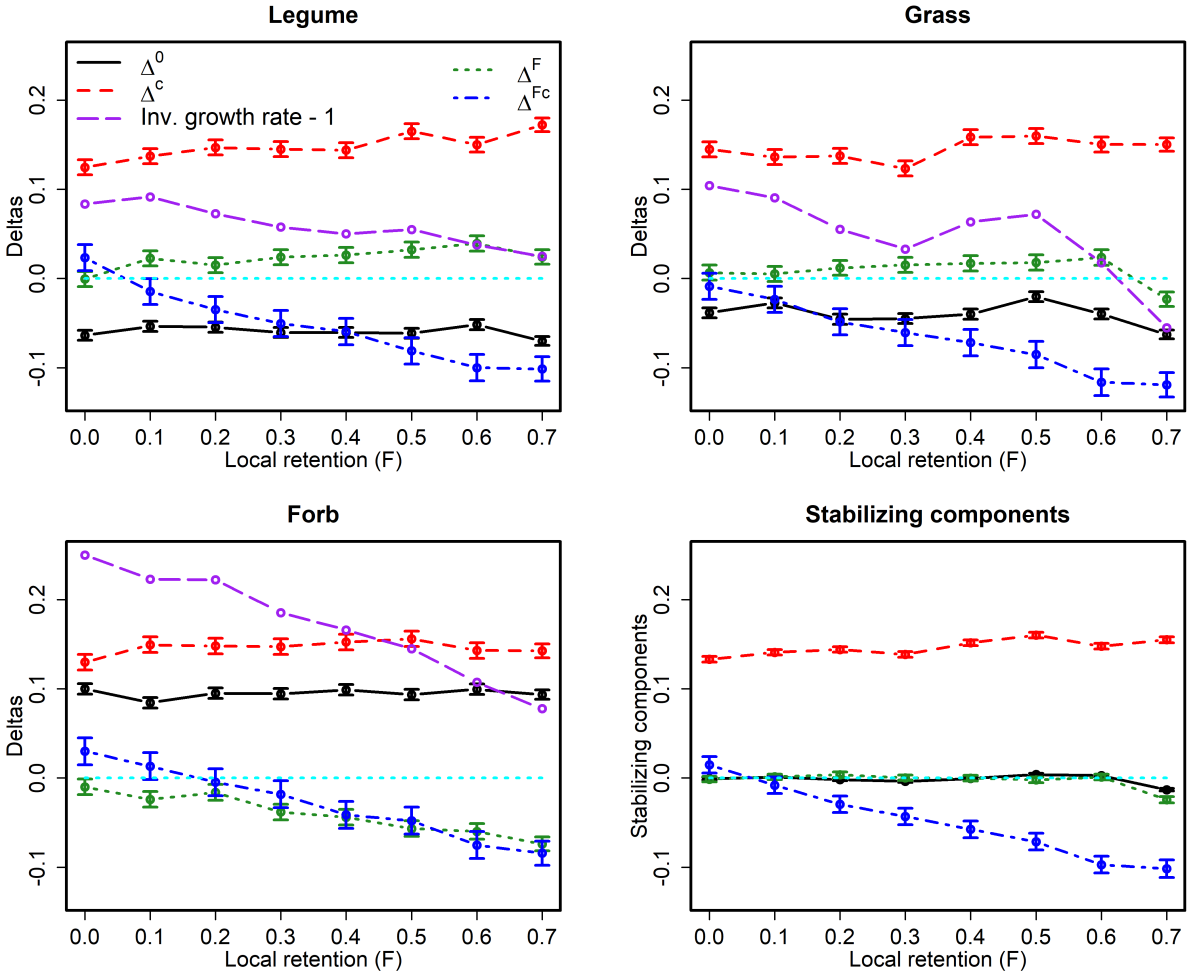

Figure 3: Strength of coexistence mechanisms as a function of the probability of local retention F in the plant-soil feedback model of Petermann *et al.* (2008). The dotted cyan curve at 0 is drawn to provide a visual baseline. We only consider $F \leq 0.7$ because stable coexistence is lost when F is slightly larger. Comparison with the analytic decomposition (sec. SI.8) shows that values for grass at $F = 0.7$ are slightly inaccurate, probably because one resident (legume) has very low steady state abundance. Figure generated by `PetermannPartitioning.R` and `plotPetermannDeltas.R`

In MCT for purely temporal variation (Chesson 1994), the population growth rate r_j of species j is assumed to depend on the environment, E_j, and competition, C_j. E and C are not direct measures of the physical environment and competition, but parameters that represent population responses (e.g., C may be the proportional reduction in cell division rate due to resource scarcity). Note that C includes all frequency- and density-dependent feedbacks. MCT then asks how differences among species in the distributions and impacts of the E_js and C_js affect the long-run growth rate of each species in both resident and invader states. Second-order Taylor expansion is used to partition the effects on growth rates of different moments of $\mathscr{E}_j$ and $\mathscr{C}_j$, the direct effects of E_j and C_j on growth rates. The invader-resident differences in each of the resulting terms are then grouped into the following "mechanisms" for species i as invader:

- r_i', the sum of all terms that do not include density-dependent feedbacks.
- $\Delta\rho_i$, the sum of all terms involving means of the $\mathscr{C}_j$.
- ΔN_i, the sum of all terms involving variances of the $\mathscr{C}_j$.
- ΔI_i, the sum of all terms involving $\mathscr{E}_j, \mathscr{C}_j$ covariances.

r_i' gives the invasion growth rate in the absence of direct density-dependent feedbacks. However, it includes $Var(E)$ terms that measure effects of environmental fluctuations on population growth rates, which we generally make a separate term in our analyses. Whenever environment and competition both vary, there are two possible sources of nonlinear averaging, but only one of them (competition) gets a stand-alone term in standard MCT.

$\Delta\rho_i$ represents all fluctuation-independent mechanisms ,such as resource partitioning or species-specific enemies. In standard MCT, the scaling factors q_{ir} used in invader-resident comparisons (see eqn. 20) are chosen so that $\Delta\rho_i = 0$.

ΔN_i is called *relative nonlinearity in competition*. This fluctuation-dependent term reflects differences in the degree of nonlinearity of r in each species' response to limiting competitive factors. If these differences are present, and the limiting factors fluctuate, nonlinear averaging can benefit some species and hurt others.

ΔI_i is called the *storage effect* because this mechanism's importance was first recognized in models where gains during good years were "stored" in a long-lasting life stage with low sensitivity to environment or competition. However, ΔI can make a positive contribution to coexistence whenever invaders have low environment-competition covariance (letting them increase rapidly in good conditions) and they are buffered against equally rapid decrease in bad conditions.

The canonical growth-rate decomposition for purely temporal variability is then

$$\bar{r}_i = r_i^{'} + \Delta N_i + \Delta I_i. \tag{28}$$

With spatial rather than temporal variability, there is an additional term (fitness-density spatial covariance) and the spatial storage effect involves spatial rather than temporal covariance of environment and competition.

Our growth-rate decompositions differ in several ways. Because we do not use Taylor approximations, our decompositions usually include higher-order interaction terms. Where standard MCT reduces the number of terms by grouping and weighting, we decompose finely. We also prefer to work directly with the measurable state variables and environmental covariates that characterize the community (e.g., resource concentration and temperature) rather than the effects of resource limitation and temperature on population growth rates. However, users who prefer can express population growth rates as functions of E and C variables as they would be defined in standard MCT, and do decompositions using our methods that align more closely with the canonical mechanisms. We discuss these options for our diatoms case study in sec. SI.3.

Box 1: Summary of the canonical coexistence mechanisms in MCT, following Barabás *et al.* (2018).

Supporting Information Appendix S1, Technical Details and Supplements

S.P. Ellner, R.E. Snyder, P.B. Adler & G.J. Hooker, "Expanding Modern Coexistence Theory..."

Ecology Letters

SI.1 Using Taylor series to "decompose and compare"

Here we give a somewhat simplified (as we explain at the end) illustration of how standard MCT uses Taylor series expansions to decompose population growth rates and do invader-resident comparisons.

Chesson (1994) assumes that population growth rates r depends on a competition factor $C(t)$ and a temporally varying environment factor $E(t)$. Then a second order Taylor series expansion about the means of E and C is:

$$\begin{aligned} r(E(t),C(t)) = r(\bar{E},\bar{C}) &+ \frac{\partial r}{\partial E}(E(t)-\bar{E}) + \frac{\partial r}{\partial C}(C(t)-\bar{C}) \\ &+ \frac{1}{2}\frac{\partial^2 r}{\partial E^2}(E(t)-\bar{E})^2 + \frac{1}{2}\frac{\partial^2 r}{\partial C^2}(C(t)-\bar{C})^2 \\ &+ \frac{\partial^2 r}{\partial E \partial C}(E(t)-\bar{E})(C(t)-\bar{C}) + \cdots \end{aligned} \tag{SI.1}$$

Here partial derivatives are evaluated at $\bar{E},\bar{C}$ and $\cdots$ are higher-order terms in $E-\bar{E}$ and $C-\bar{C}$. Analytic MCT makes the *small variance approximation* that these terms are small enough to ignore. Then, taking time averages of both sides in (SI.1) we have

$$\bar{r} \approx r(\bar{E},\bar{C}) + \frac{1}{2}\frac{\partial^2 r}{\partial E^2}Var(E) + \frac{1}{2}\frac{\partial^2 r}{\partial C^2}Var(C) + \frac{\partial^2 r}{\partial E \partial C}Cov(E,C). \tag{SI.2}$$

Next, to do invader-resident comparisons, we apply (SI.2) to all species in the community when species i is a rare invader and all other species $k \neq i$ are residents. Because residents have average population growth rate $\bar{r}_k = 0$, for any coefficients q_{ik} we have

$$\bar{r}_i = \bar{r}_i - \sum_{k \neq i} q_{ik}\bar{r}_k.$$

Applying (SI.2) to each $\bar{r}$ on the right-hand side of the previous equation, we have

$$\begin{aligned}\bar{r}_i \approx & \frac{1}{2}\left[\frac{\partial^2 r_i}{\partial E^2} Var(E_i) - \sum_{k\neq i} q_{ik} \frac{\partial^2 r_k}{\partial E^2} Var(E_k)\right] \\ & + \frac{1}{2}\left[\frac{\partial^2 r_i}{\partial C^2} Var(C_i) - \sum_{k\neq i} q_{ik} \frac{\partial^2 r_k}{\partial C^2} Var(C_k)\right] \\ & + \left[\frac{\partial^2 r_i}{\partial E \partial C} Cov(E_i, C_i) - \sum_{k\neq i} q_{ik} \frac{\partial^2 r_k}{\partial E \partial C} Cov(E_k, C_k)\right].\end{aligned} \tag{SI.3}$$

In eqn. (SI.3) the invaders' population growth rate is expressed as a sum of term-by-term invader-resident differences.

E and C in (SI.3) are species-specific because they often represent the effect of environment and competition on each species, rather than actual covariates such as rainfall or species abundances. Be warned, MCT uses different baseline E and C, makes a specific choice of the *scaling factors* q and takes additional steps involving Taylor-expanding Cs as functions of "limiting factors". To learn a bit about these things see Box 1, and in section SI.2 we do a complete standard MCT analysis of the model in our diatoms case study. For the full story in general, see Barabás *et al.* (2018). The point of this section is simply to illustrate how second-order Taylor approximations lead to approximations of invasion growth rates in terms of means, variances, and covariances of "parameters" measuring the impacts of environment and competition.

SI.2 Standard MCT decomposition for the diatoms case study

In this section we provide the technical details of how we carried out a standard MCT decomposition for our diatoms case study. Thus, technical familiarity with standard MCT is necessary for reading this section. However, reading this section is not necessary for understanding the final results, which are discussed in the next section below. If you're willing to trust that we did the math right, you can skip directly from here to the start of Sec. SI.3.

The first step in a Chesson-style standard MCT decomposition is to define the environment parameter, $E(t)$, and competition parameter, $C(t)$. As discussed in the previous section, the environment is not the physical environment but one or more environmentally-dependent demographic parameters — a species' response to the environment. Here the natural choice is $E(t) = V(t)$, the maximum cell division rate. As in Ellner *et al.* (2016), we choose competition $C(t) = (K_j + S(t))/S(t)$, so that per capita population growth rate

$$r_j = \frac{E_j}{C_j} - D \tag{SI.4}$$

increases with E_j and decreases with C_j.

The next step is to switch to standardized variables that express changes in environment and competition in terms of impacts on population growth rate:

$$\mathscr{E}_j = r_j(E_j, C_j^*) = \frac{E_j}{C_j^*} - D \tag{SI.5}$$
$$\mathscr{C}_j = -r_j(E_j^*, C_j) = D - \frac{E_j^*}{C_j},$$

where the baseline values E_j^* and C_j^* are constants. Chesson's formalism is valid when environmental fluctuations about E_j^* are small, so E_j^* is typically taken to be the mean value of E: $E_j^* = \langle V_j \rangle_t$. The constant C_j^* is defined by $r_j(E_j^*, C_j^*) = 0$, so in our case, $C_j^* = E_j^*/D$.

We also require two constants, the scaling factors q_{ir} and γ. Because there is only a single competitive factor, silicate, we can use the definition

$$q_{ir} = \left.\frac{d\mathscr{C}_i}{d\mathscr{C}_r}\right|_{\mathscr{C}_r=0} = \left.\frac{d\mathscr{C}_i}{dS}\left(\frac{d\mathscr{C}_r}{dS}\right)^{-1}\right|_{S=K_r/(C_r^*-1)} = \left.\frac{E_i^* K_i}{(K_i+S)^2}\frac{(K_r+S)^2}{E_r^* K_r}\right|_{S=K_r/(C_r^*-1)}. \tag{SI.6}$$

Our other constant is γ_j, which represents the degree to which the effects of environment and competition are non-additive:

$$\gamma_j = \left.\frac{\partial^2 r_j}{\partial \mathscr{E}_j \mathscr{C}_j}\right|_{\mathscr{E}_j=\mathscr{C}_j=0} = \frac{dC_j}{d\mathscr{C}_j}\frac{\partial}{\partial C_j}\left(\frac{\partial r_j}{\partial E_j}\frac{dE_j}{d\mathscr{E}_j}\right)\Bigg|_{E_j=E_j^*,\ C_j=C_j^*} = -\frac{1}{D}, \tag{SI.7}$$

where we have used the fact that $E_j^*/C_j^* = D$.

Standard MCT first makes a small variance approximation to write

$$\bar{r}_j \approx \langle \mathscr{E}_j \rangle_t - \langle \mathscr{C}_j \rangle_t + \gamma_j \, Cov(\mathscr{E}_j, \mathscr{C}_j)_t, \tag{SI.8}$$

and writes $\bar{r}_i = \bar{r}_i - q_{ir}\bar{r}_r$ as a term-by-term comparison. The difference of the covariance terms is called the storage effect (see Box 1):

$$\begin{aligned} \Delta I &= \gamma_i \, Cov(\mathscr{E}_i, \mathscr{C}_i) - q_{ir}\gamma_r \, Cov(\mathscr{E}_r, \mathscr{C}_r) \\ &= \frac{1}{D}\frac{E_i^*}{C_i^*} \, Cov\left(E_i, \frac{1}{C_i}\right) - q_{ir}\frac{1}{D}\frac{E_r^*}{C_r^*} \, Cov\left(E_r, \frac{1}{C_r}\right) \\ &= Cov\left(E_i, \frac{1}{C_i}\right) - q_{ir} \, Cov\left(E_r, \frac{1}{C_r}\right), \end{aligned} \tag{SI.9}$$

where we have again used the fact that $E_j^*/C_j^* = D$.

Rather than working with $\langle \mathscr{E}_j \rangle_t$ and $\langle \mathscr{C}_j \rangle_t$, standard MCT then makes a second small variance approximation, expanding $\mathscr{C}_j$ to second order around $C_j = C_r^*$:

$$\langle \mathscr{C}_j \rangle_t \approx \mathscr{C}_j(C_j = C_r^*) + \left.\frac{d\mathscr{C}_j}{dC_j}\right|_{C_r^*} (C_j - C_r^*) + \frac{1}{2} \left.\frac{d^2\mathscr{C}_j}{dC_j^2}\right|_{C_r^*} (C_j - C_r^*)^2. \tag{SI.10}$$

We now substitute this expansion into $\langle \mathscr{C}_i \rangle_t - q_{ir} \langle \mathscr{C}_r \rangle_t$. The choice of q_{ir} makes the invader and resident linear terms cancel out. The constant term is zero for the resident, while the invader constant term is combined with $\langle \mathscr{E}_i \rangle_t - q_{ir} \langle \mathscr{E}_r \rangle_t$ to form

$$\bar{r}' = \langle \mathscr{E}_i \rangle_t - q_{ir} \langle \mathscr{E}_r \rangle_t - \mathscr{C}_i(C_r^*) = -\mathscr{C}_i(C_r^*) = -\left(D - \frac{E_i^*}{C_r^*}\right). \tag{SI.11}$$

(Note that in our model, $\langle \mathscr{E}_j \rangle_t = 0$ because population growth rate r_j is linear in the environment E_j, so that $\langle \mathscr{E}_j \rangle_t = r_j(\langle E_j \rangle_t, C_j^*) = r_j(E_j^*, C_j^*) = 0$.)

Finally, the quadratic terms give us relative nonlinearity of competition:

$$\begin{aligned} \Delta N &= \frac{1}{2} \left.\frac{d^2\mathscr{C}_i}{dC_i^2}\right|_{C_i = C_r^*} Var(C_i) - q_{ir} \frac{1}{2} \left.\frac{d^2\mathscr{C}_r}{dC_r^2}\right|_{C_r = C_r^*} Var(C_r) \\ &= \frac{1}{2} \left(-\frac{E_i^*}{C_r^{*3}}\right) Var(C_i) - \frac{1}{2} q_{ir} \left(-\frac{E_r^*}{C_r^{*3}}\right) Var(C_r). \end{aligned} \tag{SI.12}$$

The results of the Chesson decomposition are in Table SI-1 and are discussed in the following section. However, we note here that for the choices we have made in this example, Chesson's partitioning is substantially incomplete; that is, the sum of the terms should equal the invasion growth rate for each species, but it doesn't (Table SI-1). This comes about because of the Taylor expansion about C_r^* in eq. SI.10. Demanding that E_j have small fluctuations about E_j^* ensures that C_j will also have small fluctuations about C_j^* (Chesson, 1994). However, for the Taylor expansion of $\mathscr{C}_i$ to be accurate, we must also have small fluctuations of C_i about C_r^*, which will be true if $C_i^* \approx C_r^*$. That is not true for the choices we have made. The formulas above give $C_1^* = 4.41, C_2^* = 3.06$ regardless of which is the invader. It is possible that some other choices could be made that would keep fluctuations in E_j close to E_j^* while bringing C_i^* closer to C_r^*, but we have not explored this.

SI.3 Alternative decompositions for the diatoms case study

Our approach lets users choose which features to use in invasion growth rate decompositions, and different choices lead to different decompositions. Different decompositions are equally valid in the sense that they express an invasion growth rate as a set of main effects and interaction

terms whose sum is exactly the invasion growth rate. However, some decompositions may be more informative than others. Here we compare a set of decompositions, including ours from the main text and standard MCT from sec. SI.2, to illustrate how the decomposition is affected by the choice of variables yet all of them lead to the same biological interpretation of how fluctuating temperatures maintain species coexistence in the experiments.

Table SI-1: E-decompositions of coexistence mechanisms for experiments with two diatom species (Descamps-Julien & Gonzalez, 2005). The top decomposition is the one in the main text, based on temperature θ and silicate S. The second (below dashed line) is based on $E = V(\theta)$ and $C = (K+S)/S$; because r is linear in E, variance in E necessarily has zero main effect and zero interaction effect. The third is also based on based on $E = V(\theta)$ and $C = (K+S)/S$ but expands about $E_j^* = \langle V_j(\theta)\rangle_t$ and C_j^* chosen so that population growth rate $r_j(E_j^*, C_j^*) = 0$, as in MCT. The fourth is the standard MCT analytic decomposition presented in section SI.2. The first two decompositions use equal weighting (equivalent to setting the scaling factors in standard MCT to $q_{ir} = 1$) and the third and fourth uses the standard MCT scaling factors, in this case $q_{12} = 1.1, q_{21} = 0.89$. For comparison, in the first and second decompositions we also report values (where they differ) using the standard MCT scaling factors; table entries a/b are (equal weighting)/(standard MCT scaling factors).

Growth rate contributions	*Fragilaria* $r_{inv} = 0.061$ d^{-1}	*Cyclotella* $r_{inv} = 0.007$ d^{-1}	Stabilizing component
Fluctuation-free growth rate, Δ^*	-0.031	0.041	0.005
Fluctuation-driven change in mean S, Δ'	0.020/-0.006	0.001	0.011/-0.002
Relative nonlinearity in temperature θ, Δ^θ	0.092/0.102	-0.037	0.028/0.033
Relative nonlinearity in silicate S, Δ^S	-0.014/0.004	-0.001	-0.007/0.001
θ, S variance interaction, $\Delta^{(\theta \# S)}$	-0.045/-0.050	0.000	-0.022/-0.025
Storage effect (temperature-silicate covariance), $\Delta^{(\theta S)}$	0.038/0.042	0.003	0.021/0.022
Sum of the above:	*0.061*	*0.007*	
Fluctuation-free growth rate, Δ^*	-0.031	0.041	0.005
Fluctuation-driven change in mean E and C, Δ'	0.026	-0.036	-0.005
Relative nonlinearity in competition C, Δ^C	0.028/0.025	0.000	0.014/0.012
Storage effect (E, C covariance), $\Delta^{(EC)}$	0.038/0.042	0.003	0.021/0.022
Sum of the above:	*0.061*	*0.007*	
Relative nonlinearity in competition C, Δ^C	0.019	0.004	0.012
Storage effect (E, C covariance), $\Delta^{(EC)}$	0.042	0.003	0.022
Sum of the above:	*0.061*	*0.007*	
Fluctuation-independent, $\bar{r}'$	0.040	-0.027	0.006
Relative nonlinearity of competition, ΔN	-0.037	0.001	-0.018
Storage effect ($\mathscr{E}, \mathscr{C}$ covariance), ΔI	0.042	0.003	0.022
Sum of the above:	*0.044*	*-0.024*	

Values were calculated from the last 1200 days of a 3600 day simulation, recording 10 values each day. Growth rate contributions (Δ) are invader-resident pairwise differences in the decompositions of invader and resident growth rates. Values calculated by `ForcedChemo_Func_Covar.R`, `ForcedChemo_Chesson-C.R`, `ForcedChemo_Chesson-EC.R`, `classicChessonChemostat.R`, and `ForcedChemoSubs.R`

We prefer to work directly with the measureable factors affecting population growth rates, in this case temperature θ and silicate concentration S. Standard MCT uses environment and competition "parameters" E and C which measure the impact of environment state and other species on the focal species' population growth rate. For example, Chesson (2000a, pp. 212-213) writes (in the context of a spatial model)

> E_{jx} is called an environmentally-dependent parameter and is not a direct measure of the physical environment, but a population parameter that depends on the physical environment, such as a survival probability, a germination probability, or an expected number of offspring. . . . In most cases, it is defined so that larger values of $E_{j,x}$ mean more favorable environments.

Similarly C is some measure of the total effect of competition on the population growth rate of the focal species, defined so that larger values of C result in lower population growth rates. For the diatoms case study, the most natural choice of E is $V(\theta)$, maximum cell division rate as a function of temperature (transformations of V, such as $\log(V)$, are really the only alternative that fits the criteria). For C there are several possible choices; here and in Ellner *et al.* (2016) we use $C = (K + S)/S$ so that the population growth rate is $r = E/C - D$.

In comparing decompositions, it is important to remember that differences among them are constrained in several ways.

1. The terms always have the same sum, the invasion growth rate of the species. (This is exactly true with our approach, and approximately true for standard MCT using small-variance approximations.) This means that an effect quantified by some term cannot just disappear when we change to another decomposition where that term is absent — the effect has to show up in the other decomposition, somewhere.
2. The completely no-fluctuations baseline is always the same, because the effect of setting temperature to its mean value is independent of the subsequent steps. (Note, only the first two decompositions use this baseline.)
3. The storage effect term is always the same (exactly the same in our decomposition, and approximately the same for standard MCT). The storage effect term is the effect of de-correlating environment and competition, leaving all else untouched. In this example $E = V(\theta)$ is only a function of temperature and C is only a function of silicate (for any reasonable choice of C, not just the one we have chosen). So de-correlating θ and S is the same as de-correlating θ and C is the same as decorrelating E and C is the same as de-correlating the transformed parameters $\mathscr{E}$ and $\mathscr{C}$ that are used to define the storage effect in standard MCT (sec. SI.2).

The first decomposition in Table SI-1 is our analysis in the main text, a two-way decomposition in which all possible terms are nonzero for at least one of the species, which is typical.

Our decomposition shows the error behind our previous guess (Ellner *et al.*, 2016). There we argued that if storage effect isn't enough to explain the fluctuation-dependent coexistence of the species, the burden fell to relative nonlinearity in competition (Δ^C or Δ^S) because that's the only other fluctuation-dependent mechanism in standard MCT. We forgot about the direct effects of temperature fluctuations ("direct" meaning that they are not mediated through the resulting fluctuations in silicate). In standard MCT that contribution comes from the $\langle \mathscr{E}_i \rangle_t - q_{ir} \langle \mathscr{E}_r \rangle_t$ portion of $\bar{r}'$, a fact concealed by $\bar{r}'$'s usual description as "fluctuation-independent coexistence mechanisms." Our decompositions break out direct temperature effects as separate terms (Δ^θ and $\Delta^{(\theta \# S)}$), and those terms can also contribute to pulling $\bar{r}_i$ above zero.

The second decomposition, closer to standard MCT, has fewer terms because r is linear in E. So average growth rate at $E(t) \equiv \overline{E}$ is the same as average growth rate with a fluctuating E, regardless of whether C is constant or variable. Consequently Δ^E and $\Delta^{(E \# C)}$ are both zero, simply as a result of how E is defined. But the remaining effects must be equal:

$$\Delta' \text{ (1st decomposition) } + \Delta^\theta + \Delta^S + \Delta^{(\theta \# S)} = \Delta' \text{ (2nd decomposition) } + \Delta^C. \tag{SI.13}$$

Our third decomposition is a more accurate version of standard MCT. Like MCT, we expand E_j and C_j around E_j^* and C_j^*, where $E_j^* = \langle V_j(\theta) \rangle_t$ and C_j^* is chosen so that population growth rate $r_j(E_j^*, C_j^*) = 0$. This is in contrast to the second decomposition, in which we expanded about $V_j(\langle \theta \rangle_t)$ and $C_j(\langle \theta \rangle_t)$. Unlike MCT, however, we evaluate terms through simulations, so we do not need to assume small variance and we do not need to assume $C_i^* \approx C_r^*$. The small number of terms in this decomposition is a result of the choices above. The fluctuation-free growth rate Δ^* is necessarily zero because the fluctuation-free baseline for each species was chosen to make that true, so it is omitted from the Table. And again, Δ^E and $\Delta^{(E \# C)}$ are both zero because the E parameter was defined that population growth rates $r_j(E_j, C_j)$ are linear functions of E_j.

The fourth decomposition is standard MCT, derived in Sec. SI.2. Comparing this with the previous decomposition, we see that $\Delta^{(EC)} = \Delta I$; however, the remaining terms are not equal, and in fact the sum of the MCT terms does not equal the invader growth rate for either species. As discussed in Sec. SI.2, MCT requires two approximations. First, MCT makes a small variance approximation to write

$$\bar{r}_i \approx \langle \mathscr{E}_i \rangle_t - \langle \mathscr{C}_i \rangle_t + \gamma \, Cov(\mathscr{E}_i, \mathscr{C}_i)_t, \tag{SI.14}$$

which equals 0.061 for *Fragillaria* and 0.007 for *Cyclotella*. At this point, the MCT decomposition and our third decomposition agree, which means that the small variance approximation is a good one. Then, MCT expands $\mathscr{C}_i$ to second order about C_r^*:

$$\langle \mathscr{C}_i \rangle_t \approx \mathscr{C}_i(C_i = C_r^*) + \left. \frac{d\mathscr{C}_i}{dC_i} \right|_{C_r^*} (C_i - C_r^*) + \frac{1}{2} \left. \frac{d^2\mathscr{C}_i}{dC_i^2} \right|_{C_r^*} (C_i - C_r^*)^2. \tag{SI.15}$$

This Taylor expansion requires $C_i^* \approx C_r^*$, which is not true for our model and is the source of the discrepancy: $\langle \mathscr{C}_i \rangle_t$ = -0.058 (-0.005) for *Fragillaria (Cyclotella)*, but the right hand side of eq. SI.15 is -0.088 (0.027).

SI.4 General functional decomposition of population growth rates and invasion growth rates

Let $\mathcal{F}$ be the set of chosen features. The decomposition of population growth rate $\bar{r}$ consists of terms $\varepsilon^{\mathcal{S}}$ for all possible subsets $\mathcal{S}$ of $\mathcal{F}$, including the empty set $\mathcal{S} = \emptyset$, and the complete set $\mathcal{S} = \mathcal{F}$. The qualifier "possible" is necessary because some combinations of features may be impossible, for example covariance between X and Y can only be present if variance in X and in Y are both present. We use the notation $\mathcal{A} \subseteq^* \mathcal{B}$ to indicate that $\mathcal{A}$ is a possible subset of $\mathcal{B}$, and $\mathcal{A} \subset^* \mathcal{B}$ to denote $\mathcal{A}$ is a possible subset of $\mathcal{B}$ but not $\mathcal{B}$ itself.

For species j when species k (possibly equal to j) is the invader, let $\bar{r}^{\mathcal{S}}_{j\backslash k}$ be the long-term population growth rate of species j when the features in $\mathcal{S}$ are present and all others are absent. The decomposition starts with $\varepsilon^{\emptyset}$, the "null" population growth rate $\bar{r}^{\emptyset}_{j\backslash k}$ when the direct effects of all features of interest have been removed. Then for every nonempty possible subset $\mathcal{S}$ of $\mathcal{F}$, define

$$\varepsilon^{\mathcal{S}}_{j\backslash k} = \bar{r}^{\mathcal{S}}_{j\backslash k} - \sum_{\mathcal{A} \subset^* \mathcal{S}} \varepsilon^{\mathcal{A}}_{j\backslash k}. \tag{SI.16}$$

This definition has to implemented sequentially, first computing the terms for all possible subsets with one element, then for all possible subsets with 2 elements, and so on.

Setting $\mathcal{S} = \mathcal{F}$ in (SI.16), we have in particular

$$\varepsilon^{\mathcal{F}}_{j\backslash k} = \bar{r}^{\mathcal{F}}_{j\backslash k} - \sum_{\mathcal{S} \subset^* \mathcal{F}} \varepsilon^{\mathcal{S}}_{j\backslash k}. \tag{SI.17}$$

Re-arranging (SI.17) and noting $\bar{r}^{\mathcal{F}}_{j\backslash k} = \bar{r}_{j\backslash k}$ we obtain the general decomposition of population growth rate

$$\bar{r}_{j\backslash k} = \sum_{\mathcal{S} \subseteq^* \mathcal{F}} \varepsilon^{\mathcal{S}}_{j\backslash k}. \tag{SI.18}$$

Finally, the functional decomposition of invasion growth rates into terms $\Delta^{\mathcal{S}}$ consists of term-by-term invader-resident differences using one of the resident weightings in eqn. (20).

SI.5 Another decomposition of purely spatial coexistence mechanisms

The coexistence mechanisms for spatially varying environments (Chesson, 2000a) were analyzed in the main text by first isolating growth-density covariance as a separate term, and then using the two-factor version of our functional/covariance decomposition. Here we outline an alternate decomposition, based on a three-factor decomposition.

The starting point is the first equality in Chesson (2000a, eqn. 7) for the growth rate $\tilde{\lambda}$ of each species' total population in all patches. Using the notation from the main text, and again writing out the spatial average, the equation is

$$\tilde{\lambda}_j(t) = \frac{1}{Q}\sum_{x=1}^{Q} \nu_{j,x}(t)\lambda_j(E_{j,x}(t), C_{j,x}(t)). \tag{SI.19}$$

In (SI.19) ν, E and C have *spatial* variances and covariances, which can be treated exactly like the temporal variances in the chemostat case study. We eliminate variance in any variable by setting it to its spatial average in (SI.19), for example

$$\frac{1}{Q}\sum_{x=1}^{Q} \nu_{j,x}(t)\lambda_j(\tilde{E}_j(t), \tilde{C}_j(t)) \tag{SI.20}$$

has spatial variance only in ν ($\tilde{E}_j = \frac{1}{Q}\sum_x E_{j,x}(t)$ and similarly for $\tilde{C}_j$). For the covariance decomposition, spatial covariance among variables is eliminated by putting different spatial indices on their xs. For example, all spatial covariances are eliminated in

$$\tilde{\lambda}_j^{(\nu,E,C)}(t) = \frac{1}{Q^3}\sum_{x_1=1}^{Q}\sum_{x_2=1}^{Q}\sum_{x_2=1}^{Q} \nu_{j,x_1}(t) r_j(E_{j,x_2}(t), C_{j,x_3}(t)) \tag{SI.21}$$

As always, Δs are defined as the difference between corresponding terms for invading and resident species. As in the main text, with data (or simulations) at multiple time points, the decomposition would be done for each time point, and values of each term averaged over time.

SI.6 Trait variation *per se* in a T-decomposition

In this section we consider (only to reject) the analog for a T-decomposition of the covariance step in an E-decomposition of invasion growth rates. Any term in a T-decomposition involves comparing long-run population growth rates when each species is assigned the across-species mean with the same rate when each species is assigned its true value. This change adds trait variation and covariation (i.e., non-independence) between trait value and species identity. The

intermediate step — trait variation *per se* — allows the trait to vary across species, but each species gets a random draw (without replacement) from the set of trait values for all species, and we average population growth rates across the outcomes for all such random trait assignments.

For example, consider an intermediate step in which trait X goes from $\overline{X}$ to a random draw. Let Θ^* denote all other variables affecting population growth rate (including other traits and abiotic and biotic factors). The marginal effect of the change in trait X on the population growth rate is

$$\mathbb{E}_\Theta \, \mathbb{E}_X^\# \, r(X, \Theta^*) - \mathbb{E}_\Theta \, r(\overline{X}, \Theta^*), \tag{SI.22}$$

where the first term is the expectation over random permutation of the set of actual X values across species. That is, $\mathbb{E}_X^\# \, r(X, \Theta^*) = S^{-1} \sum_{j=1}^{S} r(X_j, \Theta^*)$, where X_j is the trait value of species j and S is the number of species.

We could in theory use such a step to decompose joint variation of traits into the effects of their joint variation *per se* and the effect of their covariation within a species, perhaps because of life history tradeoffs. For example, in the diatom case study, we could write $\varepsilon^{VK} = \varepsilon^{(V,K)} + \varepsilon^{(VK)}$, where the effect of variation in V and K *per se* is

$$\bar{\varepsilon}^{(V,K)} = \frac{1}{S^2} \sum_{j=1}^{S} \sum_{k=1}^{S} \mathbb{E}_\Theta \, r(V_j, K_k, \Theta) - (\varepsilon^0 + \varepsilon^V + \varepsilon^K), \tag{SI.23}$$

and the effect of covariance between V and K in a given species is

$$\bar{\varepsilon}^{(VK)} = \mathbb{E}_\Theta \, r(V, K) - \varepsilon^{(V,K)}. \tag{SI.24}$$

However, $\varepsilon^{(V,K)}$ will be the same for the invader and resident species. So when residents are equally weighted in the invader-resident comparison, the resident weights sum to 1 and therefore $\varepsilon^{(V,K)}$ will be zero. Because we emphasize equal weighting of residents, we do not pursue this intermediate step in the T-decomposition.

SI.7 Scaling factors q_{ir} for the beach grass model

The beach grass model is an example of the linear additive model defined and analyzed in Chesson (1994) with population densities x_j as the limiting factors F_j, but to be self-contained we derive the scaling factors for this particular model directly.

We used the notation that a subscript $j\backslash k$ indicates a value for species j in a situation where species k is absent. For the beachgrass model, the definitions of the standard parameters in

Chesson (1994) give

$$\mathscr{C}_{j\backslash i} = \frac{r_j}{K_j}\sum_{s\neq i}\alpha_{js}x_s = \sum_{s\neq i}a_{js}x_s \tag{SI.25}$$

where $a_{js} = \alpha_{js}r_j/K_j$.

Let $\mathbf{A}$ denote the matrix of a values (`A[j,s]`$= a_{js}$). Letting i be the index of the invading species, let $\mathbf{A}_{(-i)}$ be $\mathbf{A}$ with the i^{th} row and i^{th} column deleted, and $\vec{x}_R$ the vector of densities for all of the resident species $s \neq i$. Then by (SI.25) the vector $\vec{\mathscr{C}}_{R\backslash i}$ of $\mathscr{C}$ values for the resident species is $\vec{\mathscr{C}}_{R\backslash i} = \mathbf{A}_{(-i)}\vec{x}_R$ and therefore

$$\vec{x}_R = \mathbf{A}^{-1}_{(-i)}\vec{\mathscr{C}}_{R\backslash i}. \tag{SI.26}$$

Let $\phi_{(-i)}$ denote the i^{th} row of $\mathbf{A}$ with the i^{th} entry deleted, as a row vector. Then substituting (SI.26) into (SI.25),

$$\mathscr{C}_{i\backslash i} = \phi_{(-i)}\mathbf{A}^{-1}_{(-i)}\vec{\mathscr{C}}_{R\backslash i} \tag{SI.27}$$

The scaling factors q_{ir} for species i are therefore the entries of the vector $\phi_{(-i)}\mathbf{A}^{-1}_{(-i)}$ with successive values corresponding to resident species in their sequence in the matrix $\mathbf{A}$. For the model parameter values used in the main text, the scaling factor values are (with 1=AA, 2=AB, 3=EM)

$$\begin{pmatrix} * & -0.172 & 0.041 \\ 1.059 & * & 0.054 \\ 1.155 & 4.728 & * \end{pmatrix}. \tag{SI.28}$$

SI.8 Detailed methods for the Petermann et al. (2008) model

The Petermann *et al.* (2008) model is grid-based, spatially implicit, and stochastic. There are three species and N sites, each of which holds exactly one plant at census times $t = 0, 1, 2, \cdots$. Each plant produces a Poisson-distributed number of seeds, with mean R (assumed to be the same for all plants, in all three species). Each seed is locally retained in its parent's site with probability F, and with probability $1 - F$ is dispersed randomly in a spatially uniform way across all other sites. The number of dispersed seeds of species i arriving to any one site is therefore Poisson-distributed, with mean $(1 - F)R$ times the fraction of sites occupied by species i parents.

Adults then suffer random mortality. Adults die, leaving a vacant site, with species-specific probability d_i. Seeds at vacant sites compete lottery-style to occupy the site. Because of plant-soil feedbacks, a seed's weighting in the lottery depends both on the seed's species and on which species of parent had been occupying the site. If s_i is the total number of seeds of species $i = 1, 2, 3$ contending for the site vacated by mortality of a species j, the probability that species i

captures the site is

$$\frac{c_{ij}s_i}{\sum_{m=1}^{3} c_{mj}s_m}. \tag{SI.29}$$

It is always the case that $c_{ij} = 1$ for $i \neq j$ and that $c_{ii} \leq 1$. Janzen-Connell effects in species i were modeled by setting $c_{ii} = 0.5$, based on experiments comparing plant growth in soil taken from under conspecific versus allospecific established plants.

SI.8.1 Population growth rates

We now derive the population growth rates $\widetilde{\lambda}_j$ in enough generality that the $\widetilde{\lambda}$ values in Table 4 can be computed. This is mostly just bookkeeping and algebra.

In every scenario that arises in the analysis, all species have the same F value and the same c_{ii} value. To simplify notation, let $h = c_{ii}$, so h is the home-soil competitive disadvantage. Let ϕ_j be the fraction of the N sites occupied by species j. The various $\widetilde{\lambda}$ values in Table 4 are calculated using the steady-state values of ϕ_j that hold when both focal mechanisms are present: local retention ($F > 0$) and plant-soil feedbacks ($c_{ii} = 0.5$). For now we assume that these are known; at the end of this section we explain how to calculate them for each invader-resident comparison.

Let $Pois(\mu)$ denote a Poisson random variable with mean μ. We are interested in the infinite-sites limit, so we can assume that (for example) the fraction of sites vacated by death of a species 2 occupant is exactly $\phi_2 d_2$.

The seed dispersal process is equivalent to the following. A site occupied by species j receives $Pois(RF)$ locally retained seeds of species j, plus $Pois(\phi_j R(1-F))$ additional species j seeds dispersed from other sites, plus $Pois(\phi_k R(1-F))$ seeds from each species $k \neq j$.

We exploit the following convenient fact: if an urn is filled with independent $Pois(\mu_k)$ balls of color k, $k = 1, 2, \cdots$, and one ball is chosen at random, then the probability that it has color r is $\mu_r / \sum_k \mu_k$ (this is because the process is equivalent to putting $Pois(\sum_k \mu_k)$ balls into the urn, choosing one of them, and then coloring each ball color r with probability $\mu_r / \sum_k \mu_k$). This implies that the probability of a vacated site being taken by a particular species can be determined from the expected number of seeds of each species competing in the lottery to claim the site and the value of the home-soil disadvantage. We repeatedly use the fact that a thinned Poisson is Poisson distributed (thinning a Poisson means the following: draw X from a $Pois(\mu)$ distribution, and then toss X coins independently with success probability p and count the total number of successes; the total is Poisson with mean $p\mu$). Home-soil disadvantage is equivalent to thinning the number of seeds of the disadvantaged species, with success probability h.

For the rest of this section, j and k will be indices of the resident species, and i the index of the invader. Because the invader is rare and we will eventually let $\phi_i \to 0$, we can compute $\widetilde{\lambda}$ for the residents on assumption that $\phi_i = 0$.

Consider first resident species j. Conditional on it becoming vacant, a site with a species j former occupant (now deceased) is re-occupied by species j with probability

$$p_{jj} = \frac{hR[F + \phi_j(1-F)]}{hR[F + \phi_j(1-F)] + \phi_k R(1-F)} = \frac{h[F + \phi_j(1-F)]}{h[F + \phi_j(1-F)] + \phi_k(1-F)}. \tag{SI.30}$$

The probability of species k taking the site is therefore

$$p_{kj} = 1 - p_{jj} = \frac{\phi_k(1-F)}{h[F + \phi_j(1-F)] + \phi_k(1-F)}. \tag{SI.31}$$

Permuting indices, the probability that a site with species k former occupant (now deceased) is taken by species j is

$$p_{jk} = \frac{\phi_j(1-F)}{h[F + \phi_k(1-F)] + \phi_j(1-F)}. \tag{SI.32}$$

A fraction $d_r\phi_r$ of all sites are vacated by a resident species r death ($r = j, k$), so the new site occupancy of species j is $\phi_j(1-d_j) + d_j\phi_j p_{jj} + d_k\phi_k p_{jk}$. The growth rate $\widetilde{\lambda}_j$ is the new site occupancy divided by the old site occupancy, and thus

$$\widetilde{\lambda}_j = (\phi_j(1-d_j) + d_j\phi_j p_{jj} + d_k\phi_k p_{jk})/\phi_j = (1-d_j) + d_j p_{jj} + d_k\phi_k p_{jk}/\phi_j. \tag{SI.33}$$

The farthest-right term simplifies to be $O(\phi_k)$ not $O(\phi_k/\phi_j)$ because of the ϕ_j factor in the numerator of p_{jk}. Permuting indices in eqn. (SI.33) gives $\widetilde{\lambda}_k$.

Now consider rare invader species i. At a site it now occupies, the seed input is $Pois(FR)$ seeds of species i, and $Pois((1-F)R)$ seeds of resident species (really some seeds of species i might also disperse into the site from elsewhere, but this goes away when we let $\phi_i \to 0$). So if a site currently occupied by species i becomes vacant through mortality, species i reclaims the site with probability

$$p_{ii} = \frac{hFR}{hFR + (1-F)R} = \frac{hF}{hF + (1-F)}. \tag{SI.34}$$

Each species i individual disperses $Pois((1-F)R)$ seeds to other sites. All of these land as singletons on a site where all the other seeds are species j or k (again, not really, but the fraction of non-singletons is $O(\phi_i^2)$ so we can ignore it), and most sites receive zero invader seeds. At a site vacated by the death of resident species j, the probability of species i claiming the site is

$$p_{ij} = \frac{1}{hR[F + \phi_j(1-F)] + \phi_k R(1-F) + 1} \tag{SI.35}$$

and permuting k and j gives p_{ik}.

We next need to ask, how many sites vacated by death of a species j individual receive a seed from any one invader individual? The $Pois(R(1-F))$ seeds dispersed by that invader have probability ϕ_j of landing in a site occupied by a species j individual, and with probability d_j that occupant dies. The resulting number of sites (where one of the focal invader's seed is present, and the occupant is species j and dies) is a thinned Poisson, and therefore a Poisson, with mean $R(1-F)\phi_j d_j$. The number of such sites that it then occupies is a further thinned Poisson with mean

$$\begin{aligned} f_{ij} &= R(1-F)\phi_j d_j p_{ij} \\ &= \frac{(1-F)R\phi_j d_j}{1+hR[F+\phi_j(1-F)]+\phi_k R(1-F)} = \frac{(1-F)\phi_j d_j}{1+h[F+\phi_j(1-F)]+\phi_k(1-F)} \end{aligned} \tag{SI.36}$$

Permuting j and k in the last equation gives f_{ik}.

Adding up the expected gains and losses by each current invader individual, the expected number of species i sites at the subsequent time step, per species i site at the current time step, is

$$\mathbb{E}[\widetilde{\lambda}_i] = (1-d_i) + d_i p_{ii} + f_{ij} + f_{ik}. \tag{SI.37}$$

Now consider an invasion limit in which $N \to \infty$ and $\phi_i \to 0$ such that $\phi_i N \to \infty$. The actual number of species-i sites at the subsequent time step is the sum of $\phi_i N$ independent random variables with mean $\mathbb{E}[\widetilde{\lambda}_i]$. The actual finite population growth rate for species i is that number of sites divided by $\phi_i N$. By the Strong Law of Large Numbers, the actual finite population growth rate converges to its expectation, and we have

$$\widetilde{\lambda}_i = \mathbb{E}[\widetilde{\lambda}_i] = (1-d_i) + d_i p_{ii} + f_{ij} + f_{ik}. \tag{SI.38}$$

The various $\widetilde{\lambda}$ values listed in Table 4 are each calculated from the formulas above, using the F and $h = c_{ii}$ values specified in the right-hand column of the Table, and in all cases using the resident abundances ϕ_j, ϕ_k that hold when both mechanisms are present, so that the calculated main effects of F and c_{ii} do not include the indirect effects mediated by changes in resident abundance.

The resident abundances in the presence of both mechanisms can be calculated for any resident pair j, k by iteration. With species j and k resident, the resident species' dynamics are

$$\phi_j(t+1) = (1-d_j)\phi_j(t) + d_j\phi_j(t)p_{jj}(t) + d_k\phi_k(t)p_{jk}(t) \tag{SI.39}$$

with $\phi_k(t) = 1-\phi_j(t)$ and $p_{jj}(t), p_{jk}(t)$ given by the formulas above evaluated with both mechanisms present (F not set to 0, and $h = c_{ii} = 0.5$) and the time-t values ϕ_j and ϕ_k. The right-hand side is monotonic increasing in ϕ_j (because the more of you there are now, the more sites you will retain after mortality occurs, and the more seeds you will put out to capture vacant sites),

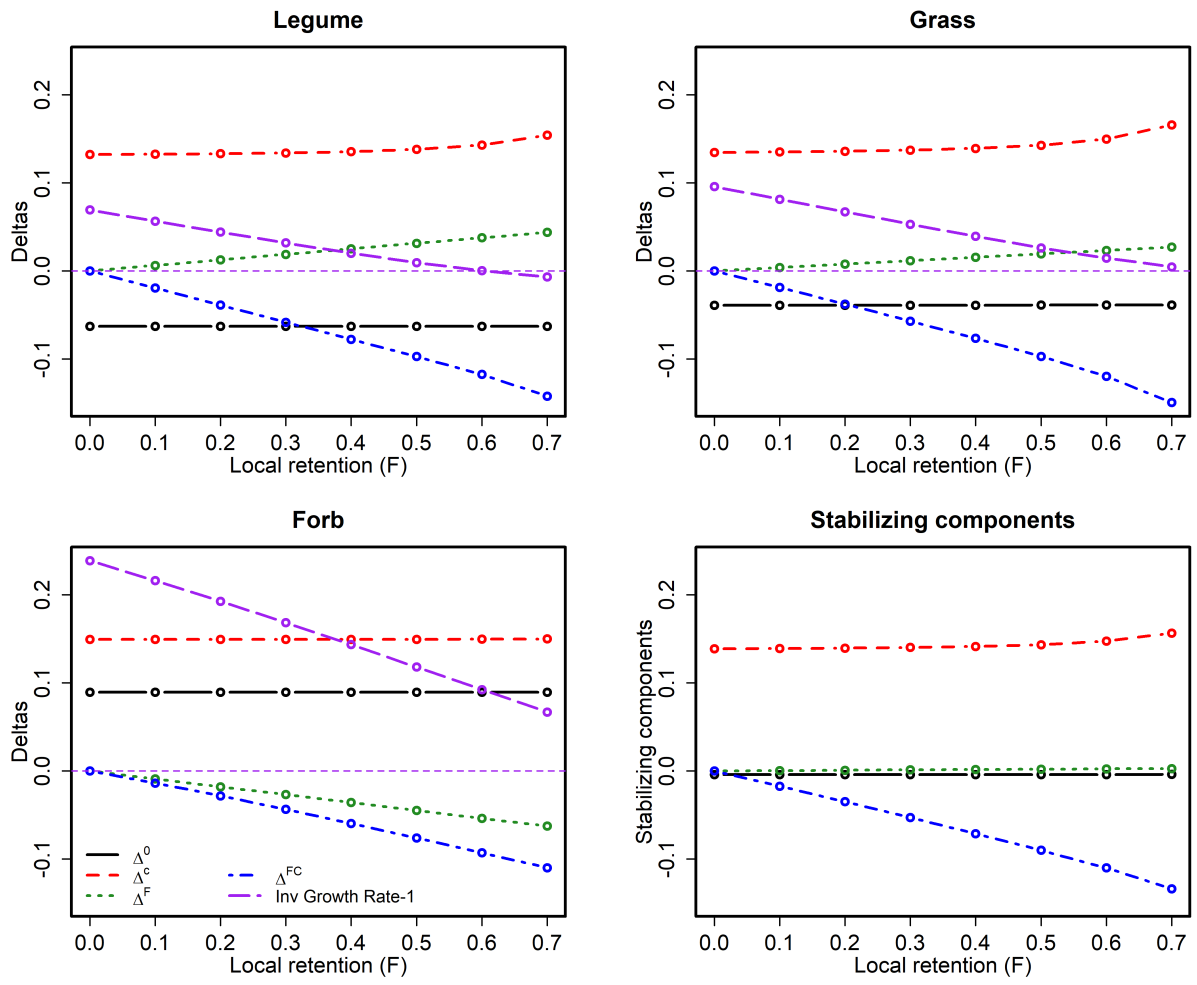

Figure SI-1: Strength of coexistence mechanisms as a function of the probability of local retention F in the plant-soil feedback model of Petermann *et al.* (2008). We only consider $F \leq 0.7$ because the three functional groups no longer coexist stably when F is slightly larger. Figure produced by `PetermannAnalytic.R`

with equilibria at $\phi_j = 0$ and $\phi_j = 1$. When the residents coexist, these will both be unstable. Without further analysis we cannot rule out the existence of multiple equilibria, so for numerical calculations we iterated (SI.39) starting from $\phi_j(0) = 0.001$ and $\phi_j(0) = 0.999$ and confirmed that both trajectories converged to the same value (within an error tolerance of 10^{-6}).

The coexistence mechanisms calculated with the formulas in this section (Fig. SI-1) confirm the accuracy of the simulation-based results shown in the main text. The only nontrivial discrepancy is for grass at $F = 0.7$. With $F = 0.7$ and both mechanisms present, one of the two residents (legume) occupies only about 3% of sites at steady state. This increases the stochasticity in simulation-based estimates because the density and $\widetilde{\lambda}$ of legume as resident are hard to estimate reliably.

SI.9 Detailed methods for the Chu & Adler (2015) IPMs

SI.9.1 Niche overlap and fitness differences

Following Chu & Adler (2015), the "no-niche" state is defined by modifying all between-species α_{ij} values (in α^R, α^S and α^G) so that each pairwise niche overlap

$$\rho = \sqrt{\frac{\alpha_{ij}\alpha_{ji}}{\alpha_{ii}\alpha_{jj}}} \tag{SI.40}$$

equals 1, without changing the fitness differences

$$\frac{\kappa_j}{\kappa_i} = \sqrt{(\alpha_{ii}\alpha_{ij})/(\alpha_{jj}\alpha_{ji})}. \tag{SI.41}$$

In a two-species Lotka-Volterra model, the species coexist if the fitness difference κ_j/κ_i, scaled by the ratio of the low-density growth rates, is between ρ and $1/\rho$ (Chesson, 2011). When $\rho = 1$, coexistence is impossible, so this is the no-niche case. We make $\rho = 1$ without altering fitness differences by changing each $\alpha_{ij}, j \neq i$ to

$$\tilde{\alpha}_{ij} = \alpha_{ij}\sqrt{\frac{\alpha_{jj}\alpha_{ii}}{\alpha_{ij}\alpha_{ji}}}, \tag{SI.42}$$

resulting in

$$\widetilde{\alpha}_{ij}\widetilde{\alpha}_{ji} = \widetilde{\alpha}_{ii}\widetilde{\alpha}_{jj} \text{ for all } i, j. \tag{SI.43}$$

SI.9.2 Models

We used exactly the models of Chu & Adler (2015). To ensure that this was the case, we began by downloading their source code provided at `dx.doi.org/10.5061/dryad.37n6f`. We then re-ran the scripts for estimating model parameter values. Full details of the model, the underlying vital rate regressions, and parameter estimation methods, are given in Chu & Adler (2015). In this section we outline the model structure, to establish notation for describing how the decomposition of invasion growth rates was done.

In the IPMs, the population of species j is represented by a density function $n_j(u,t)$ which gives the density of genets of size u at time t ("size" is natural log of genet area, so that $n_j(u,t)h$ is the number of genets whose area is between between $\exp(u)$ and $\exp(u+h)$ for $h \ll 1$). The size distribution function at time $t+1$ is given by

$$n_j(v,t+1) = \int_{L_j}^{U_j} K_j(v,u,\vec{w}_j(u,t),E_j(t))n_j(u,t)du \tag{SI.44}$$

where the kernel K_j describes all possible transitions from size u to v, $E_j(t)$ is a vector of year-specific random effects in the regression models that specify the kernel, and $\vec{w}_j(u,t)$ is a four-component vector consisting of the average crowding experienced by an individual of size u in species j from all four species in the model. The kernel is constructed from the fitted survival (S), growth (G), and recruitment (R) models,

$$K_j(v,u,\vec{w},E_j) = S_j(u,\overline{w}_j^S,E_j)G_j(v,u,\overline{w}_j^G,E_j) + R_j(v,u,\overline{w}_j^R,E_j) \tag{SI.45}$$

where $\overline{w}^V$ is the net crowding affecting process V ($V = S, G$ or R). The size interval $[L_j, U_j]$ for each species extends well beyond the range of observed sizes, to avoid unintended eviction.

The net crowding values $\overline{w}^V$ are calculated from the crowding vector $\vec{w}_j$ as

$$\overline{w}_j^V(u,t) = \sum_{k=1}^{4} \alpha_{jk}^V w_{jk}(u,t). \tag{SI.46}$$

Here $w_{jk}(\cdot,t)$ is the k^{th} component of $\vec{w}_j(\cdot,t)$, the crowding experienced by a size-u individual in species j from all individuals in species k. It is calculated from the density functions $n_j(\cdot,t)$ and $n_k(\cdot,t)$, using a mean-field approximation that captures the essential features of spatially-explicit local competition and results in larger individuals experiencing weaker intraspecific competition (Adler *et al.*, 2010; Chu & Adler, 2015).

We simulated the IPM using a kernel sampling approach (Metcalf *et al.*, 2015), as follows. Parameters for S, G and R were estimated in a Bayesian mixed-effects framework. We calculated a year-specific posterior mean for the intercept and slope parameters in each regression, for each observed transition in the data sets. To simulate a time step in the model, one year-specific parameter vector (consisting of slope and intercept parameters for all kernels in all species) was chosen at random from the set of all such parameter vectors, and was then used to calculate all kernels for all species.

For the analysis in this paper, the key aspect of model structure is eqn. (SI.46). Each of the sub-kernels S, G, and R involves a different relative weighting of intra- and inter-specific competition, characterized by the matrix of competition coefficients α_{jk}. By altering those matrices, separately or in tandem, we can determine how much the effects of niche differences on each of the corresponding demographic rates contributes to species coexistence.

SI.9.3 Outline of the decomposition

We carried out a version of the T-decomposition in which the three main effects are niche differences affecting recruitment, growth, and survival, as represented by the matrices of competition coefficients α_{ij}^V. Population growth rates with modified αs were computed using population densities and size-structures from simulations with unmodified αs. So as in other T-decompositions,

we consider only direct effects of traits, not their indirect effects through modification of the biotic environment.

The steps involved are as follows, for species j invading a community of the other three species.

1. **Simulation:** The first step is to carry out a long simulation ($t = 0$ to T) with species j absent and the others as resident. To simplify notation below we assume that the "long simulation" was preceded by a burn-in period, such that the resident community was fluctuating at its stochastic steady-state from $t = 0$ to T. The time-dependent population states $n_{k\backslash j}(t)$, crowding vector $w_{k\backslash j}(u,t)$, and environment parameters $E_k(t)$ for each resident species are stored (we use red to indicate something that was saved from the original long simulation and is being re-used). Because we use kernel selection, $E_k(t)$ can be an integer identifying which of the year-specific parameter vectors was used in year t of the original simulation.
2. **Null growth rate:** Let K_k^0 denote the kernel for species k calculated using the modified competition coefficients (SI.42) for S, G and R (so "0" indicates that niche differences are completely absent). For any state distribution $n_k(u)$ let $\|n_k\|$ be the total population $\int_{L_k}^{U_k} n_k(u)du$. The null one-step growth rates for species $k = 1, 2, 3, 4$ are calculated as

$$\lambda_{k\backslash j}^0(t) = \left\| \int_{L_k}^{U_k} K_k^0\left(v, u, \vec{w}_{k\backslash j}(u,t), E_k(t)\right) n_{k\backslash j}(u,t)du \right\| / \left\| n_{k\backslash j}(t) \right\|, \tag{SI.47}$$

   from $t = 0$ to T, where $\vec{w}_{k\backslash j}(u,t), E_k(t)$ and $n_{k\backslash j}$ are stored values from the original long simulation and $||n||$ is the total population $\int_L^U n(u)du$. The null growth rate is calculated as

$$\bar{\varepsilon}_{k\backslash j}^0 = \frac{1}{T}\sum_{k=0}^{T-1} \log \lambda_{k\backslash j}^0(t). \tag{SI.48}$$

3. **Main effects:** Let K_k^V denote the kernel for species k calculated using the true competition coefficients for subkernel V, and the modified coefficients (SI.42) for the other processes. Equation (SI.47) with K_k^V in place of K_k^0 gives one-step growth rates $\lambda_{k\backslash j}^V(t)$, and then

$$\bar{\varepsilon}_{k\backslash j}^V = \frac{1}{T}\sum_{k=0}^{T-1} \log \lambda_{k\backslash j}^V(t) - \bar{\varepsilon}_{k\backslash j}^0 \tag{SI.49}$$

4. **Two-way interactions:** Let K_k^{VW} denote the kernel for species k calculated using the true competition coefficients for subkernels V and W, and the modified coefficients (SI.42) for the other subkernel. Equation (SI.47) with K_k^{VW} in place of K_k^0 gives one-step growth rates $\lambda_{k\backslash j}^{VW}(t)$, and then

$$\bar{\varepsilon}_{k\backslash j}^{VW} = \frac{1}{T}\sum_{k=0}^{T} \log \lambda_{k\backslash j}^{VW}(t) - [\bar{\varepsilon}_{k\backslash j}^0 + \bar{\varepsilon}_{k\backslash j}^V + \bar{\varepsilon}_{k\backslash j}^W] \tag{SI.50}$$

5. **Three-way interaction:** Let K_k denote the actual kernel for species k, using the true competition coefficients in all subkernels. Use that in place of K_k^0 in eqn. (SI.47) to get one-step growth rates $\lambda_{k\backslash j}(t)$, and then

$$\begin{aligned}\bar{\varepsilon}_{k\backslash j}^{SGR} = \frac{1}{T}\sum_{k=0}^{T}\log\lambda_{k\backslash j}(t) - [\bar{\varepsilon}_{k\backslash j}^{0} + \bar{\varepsilon}_{k\backslash j}^{S} + \bar{\varepsilon}_{k\backslash j}^{G} + \bar{\varepsilon}_{k\backslash j}^{R}] \\ - [\bar{\varepsilon}_{k\backslash j}^{SG} + \bar{\varepsilon}_{k\backslash j}^{GR} + \bar{\varepsilon}_{k\backslash j}^{SR}],\ k = 1,2,3,4.\end{aligned} \tag{SI.51}$$

SI.9.4 Including indirect effects

The one-step growth rate calculations above (and the results for this model reported in the main text) use the time-dependent population structures $n_{k\backslash j}(u,t)$ stored from the original simulation. Our no-niche state thus involves removing the direct effect of niche differences (as represented by the α^V matrices) given the abiotic and biotic environments experienced by the species. However, it does not remove the indirect effects that result from how the population interactions (as represented by the α^V matrices) affect the biotic environment (abundance and population structure of each species). In doing the calculations this way, we are regarding population abundances and structures as part of the environment within which the α^V matrices determine each species' population growth rate.

Fully incorporating indirect effects is problematic, because some removals of niche differences cause one of the species (*Artemisia*) to go extinct. Invader-resident growth rate comparisons are then complicated by the fact that the set of residents depends on which niche differences are present and absent. How to properly handle such situations is "beyond the scope of this paper" – we don't want to give bad advice, and we don't want to delay this paper until we have better advice.

However, it is straightforward to include the indirect effects of α^V values on population structure. The conceptual recipe is to use the stored crowding vectors $\vec{w}_{k\backslash j}(u,t)$ from the original simulations, but simulate the changes in population structure that occur under a given set of α^V matrices. The calculations are as follows. In place of eqn. (SI.47), one-step growth population rates would be computed as follows. Let $\tilde{n} = n/\|n\|$ denote population structure scaled to have norm 1, and set $\tilde{n}_{k\backslash j}(0) = n_{k\backslash j}(0)/\|n_{k\backslash j}(0)\|$. Then for $t = 0$ to T, iterate the population structure and one-step growth rates:

$$\begin{aligned}\hat{n}_{k\backslash j}(v,t+1) &= \int_{L_k}^{U_k} K_k^0\left(v,u,\vec{w}_{k\backslash j}(u,t),E_k(t)\right)\tilde{n}_{k\backslash j}(u,t)du \\ \lambda_{k\backslash j}^0(t) &= \|\hat{n}_{k\backslash j}(t+1)\|/\|\tilde{n}_{k\backslash j}(t)\| \\ \tilde{n}_{k\backslash j}(t+1) &= \hat{n}_{k\backslash j}(t+1)/\|\hat{n}_{k\backslash j}(t+1)\|\end{aligned} \tag{SI.52}$$

The rescalings from n to $\tilde{n}$ in (SI.52) have no effect on the one-step population growth rates $\lambda_{k\backslash j}$, because the kernel is computed from the stored crowding $\vec{w}_{k\backslash j}(u,t)$. The rescaling is a precaution against the numerical underflow or overflow that could occur without the rescaling, because the iteration does not include any feedback from n to $\vec{w}$. In this version of the decomposition, competitive pressure as a function of size (which is determined by $\vec{w}$) is part of the fixed "environment" in which the species "traits" (the α matrices) affect population growth rate, but population structure $\tilde{n}$ is not: as traits vary (in constructing the decomposition), population structure of each species also varies.

Equations (SI.48) through (SI.51) then remain the same, except that the λ^V values are computed using the $\hat{n}$ values produced by the iteration (SI.52) with the appropriate kernel (e.g., K^S, K^{SG}, etc.).